DET NORSKE VIDENSKAPS-AKADEMI I OSLO

# GEOFYSISKE PUBLIKASJONER
## GEOPHYSICA NORVEGICA

Vol. XXVI. No. 12 February 1967

JACK NORDØ AND KJARTAN HJORTNÆS

# Statistical studies of precipitation on local, national and continental scales



OSLO 1966
UNIVERSITETSFORLAGET

GEOFYSISKE PUBLIKASJONER
GEOPHYSICA NORVEGICA
VOL. XXVI NO. 12

# STATISTICAL STUDIES OF PRECIPITATION ON LOCAL, NATIONAL, AND CONTINENTAL SCALES

By
Jack Nordø and Kjartan Hjortnæs

FREMLAGT I VIDENSKAPS-AKADEMIETS MØTE DEN 2. DESEMBER 1966
AV FJØRTOFT

**Summary.** Statistical studies of precipitation were undertaken on time scales ranging from 12 hours to one month. Most investigations refer to Norwegian data, but a fifty-year period of European data was also analysed by an optimal regression analysis.

The orographic release of precipitation appears to be quite dominant on all time scales in most of Norway and in Europe as well. We selected sea-level pressures as independent variables in order to derive quantitative precipitation estimates from geostrophic flow indices. The results should have practical applicability, at least until the numerical models can take proper account of vertical motions forced by mountains, even on scales of 100 km or less.

**1. Introduction.** In middle and high latitudes precipitation is abundant along the western mountain ranges of the continents. The region of maximum precipitation corresponds with the area of the largest slope of the large-scale mountain distribution. Similar regions of maximum rainfall are also found in tropical areas where upslope winds prevail.

The aim of this paper is to present quantitative relations between precipitation and the geostrophic wind component normal to large-scale mountains. Local mountains may cause deviations in this relationship, but the correlation of precipitation and large-scale onshore winds is generally high. This correlation is especially homogeneous in regions where the slope of the large-scale mountains faces into the wind, and where the forced upslope winds are predominant compared to the vertical motions in waves on synoptic scales.

BERGERON (1965) claims that even modest surface irregularities will increase the precipitation significantly. Across the Norwegian coast where a westerly current may be lifted 1–2 km, the orographic precipitation should be predominant. This feature is clearly pointed out in a series of synoptic studies by SPINNANGR *et al.* (1943, 1943, 1954, 1955). Papers by BRUUN (1944), JOHANSEN (1947), and HESSELBERG (1962) give further verification of the orographic influence.

In the following study we shall try to present more quantitative estimates of the relations between local precipitation and the pressure distribution on synoptic scales. Relations have been derived for periods ranging from 12 hours to 30 days. All statistics are derived by data analysis on the computer at the Norwegian Meteorological Institute.

Monthly precipitation records were processed for 268 stations for the period 1931–60. The observations were punched on Telex in 1963 and read and checked by computer programs developed by us. Personnel from the Division of Precipitation undertook all responsibilities in the practical procedures of punching and correcting erroneous data. Synoptic data became available in 1964. The Division of Climatology gave us the checked data on magnetic tapes.

The research reported below is taken from results derived by the general statistical computer procedures developed by NORDØ (1960). Some preliminary reports of these results have been given recently, see NORDØ (1964, 1966).

**2. Quantitative estimates of orographic precipitation.** We shall first investigate the 12-hour precipitation recorded at 18 GMT in Førde, Western Norway (Fig. 1). Fig. 2 shows the relation between precipitation and simultaneous (12 GMT) onshore geostrophic wind. The wind is proportional to the pressure difference Utsira–Hellisøy, which is the abscissa. The data sample was selected from the months of January and February, 1957–63. The precipitation is almost negligible for offshore winds (negative pressure differences) (mean, 0.3 mm). Indeed, the bulk of such precipitation was measured on just three days when quite strong onshore winds prevailed aloft, but a shallow surface trough remained along the coast at 12 GMT. Increasing onshore winds (positive differences) are associated with steadily increasing precipitation, and the mean is as high as 5.0 mm. Multiplying the pressure difference by the operator $\partial$, $\partial = 1$ for onshore winds, $\partial = 0$ for offshore winds, and carrying out a curvilinear regression analysis, we established the continous curve. It should be mentioned that most of the explained variance is given by the linear term.

Fig. 3 shows the observed frequencies of the chosen pressure difference $w$. The mean value is close to 0.9 mb, and the asymmetry is quite noteworthy. A broken curve repeats the precipitation response given in Fig. 2. The dotted curve is an exponential fit ($e^{-aw}$) to the histogram for values ranging from 0.0 mb to 7.0 mb. Using this fit and the continuous curve of Fig. 2, we can compute the probability of precipitation greater than a given bond. The tabulation in Fig. 3 shows a satisfactory correspondence with observation.

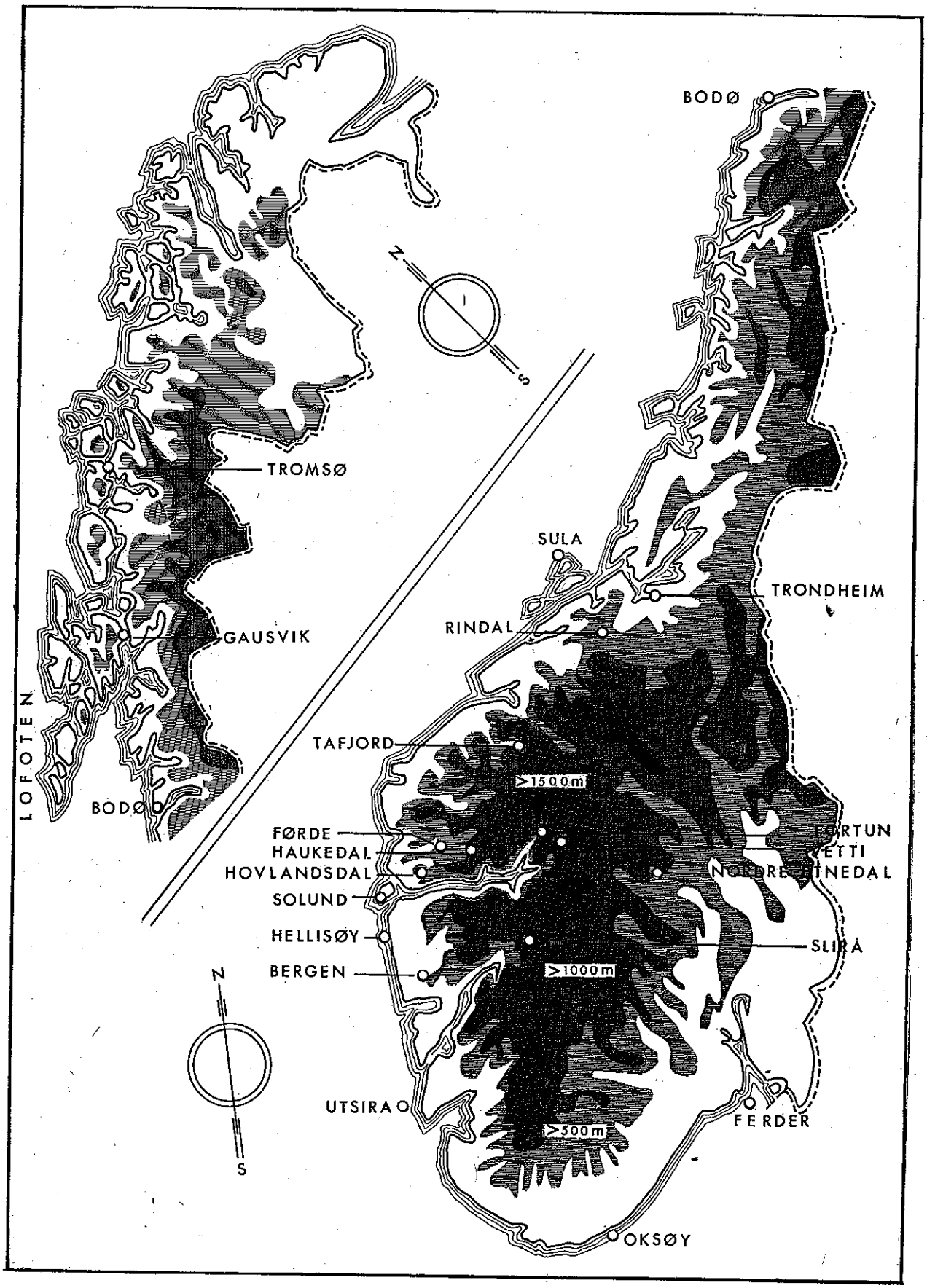


Fig. 1. Height of land in equidistances of 500 m, and location of reference stations.

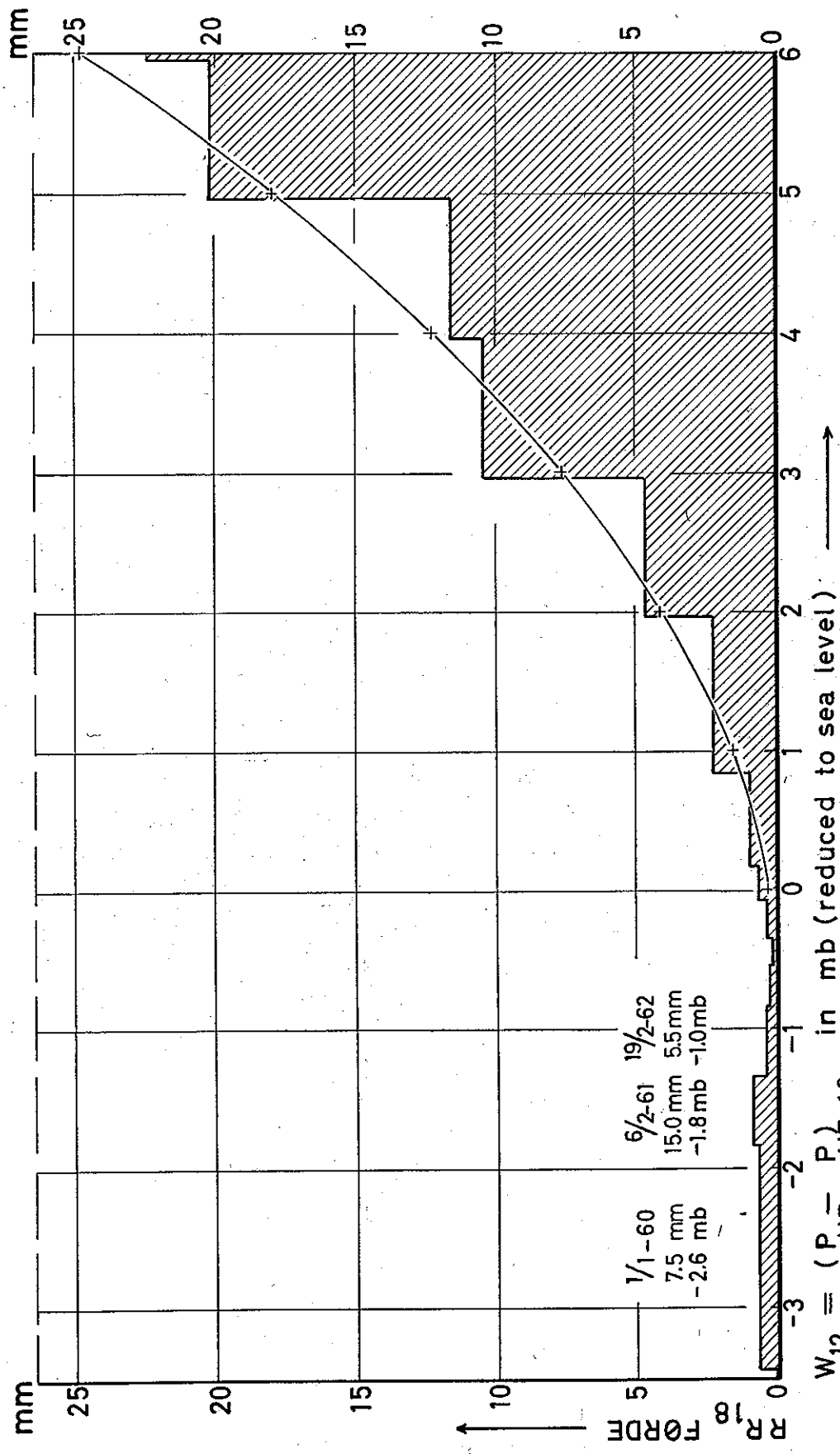


Fig. 2: 12-hours precipitation at 18 GMT in Førde as a function of the pressure difference ($p_{\text{Utsira}} - p_{\text{Hellisøy}}$) at 12 GMT.

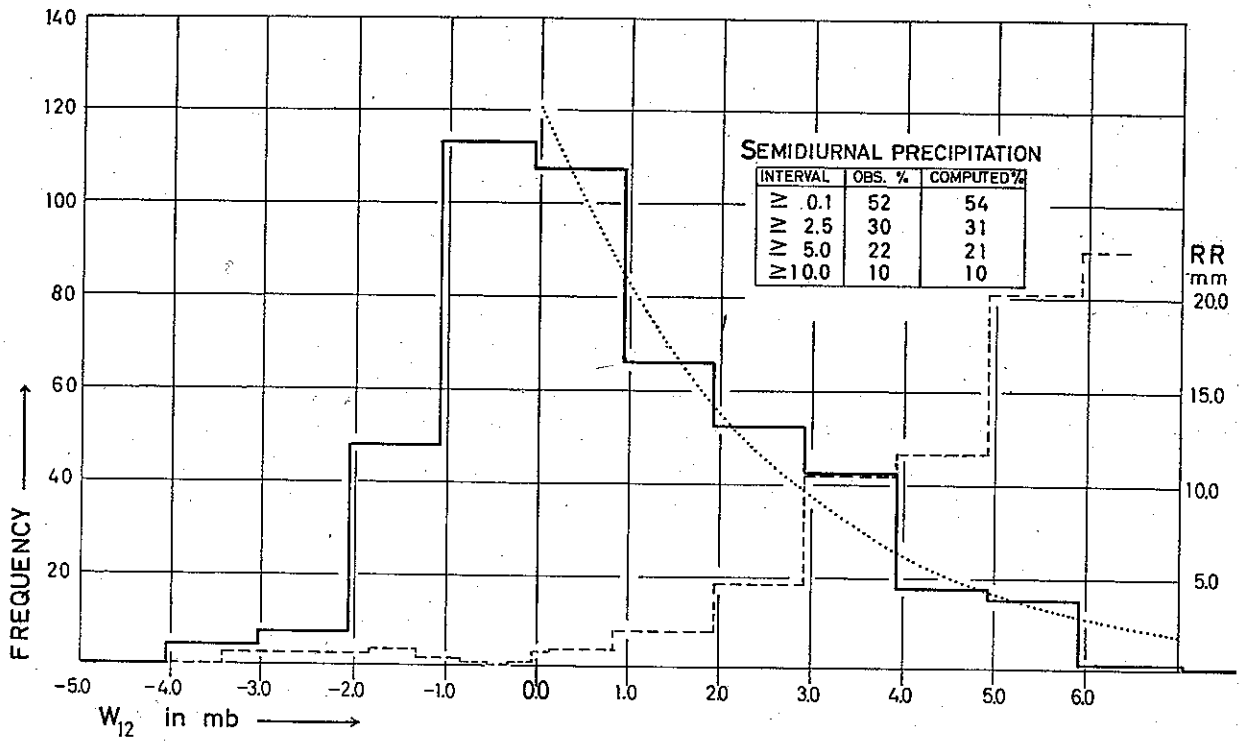


Fig. 3: Histogram of $w_{12}$ equal to $(p_{\text{Utsira}}-p_{\text{Hellisøy}})_{12}$. The dotted curve is an exponential fit. Broken lines give average precipitation for given values of $w_{12}$.

As mentioned above, there is a good linear relationship between the geostrophic onshore wind and recorded precipitation. The frequency distribution of the precipitation $RR$ should therefore be proportional to $e^{-b\,RR}$, as a first approximation. The integral $\int_{RR}^{\infty} e^{-bt}\,\mathrm{d}t = b^{-1}\,e^{-b\,RR}$ is also proportional to the same exponential. Consequently we will find $\ln P \propto -RR$, where $P$ denotes the probability of having precipitation greater or equal to $RR$. AUNE (1966) has found such relations for some Norwegian stations with rather long records.

Even though the orographic effect is predominant in most of Norway, other significant effects are always present. We neglect, e. g., vertical motions on synoptic scales, and such motions are certainly decisive at some distance from the mountains. Neither do we take the vertical shear of the flow into account. In the three cases mentioned above (see dates on Fig. 2) the surface fields were certainly misleading estimates of the vertically averaged onshore winds near Førde. Furthermore, we consider neither the moisture content nor the static stability, both of which may become very important parameters.

Such physical effects are formally noise in our study. Averaging over two or more consecutive days, using only 18 GMT records, this noise may be damped somewhat, see Fig. 4. We notice that the correlation between onshore wind and precipitation increases somewhat until we use means of 3 to 4 consecutive 18 GMT precipitations.

Then the correlation curve tapers off, and most of the remaining slow rise is probably due to the annual trend, see NORDØ (1959). Fig. 5 presents the correlation curve for the same four stations as in Fig. 4, using but $w$ instead of $\partial w$. The correlations are now, of course, lower, but the averages of values for three or more successive days give rather stable values. As Hellisøy is located at some distance from the coastal mountains, the orographic effect becomes less dominant, which is clearly illustrated by the modest correlations on both preceding diagrams.

Because averaging over 3 to 4 successive 18 GMT records gives relations similar to those found for monthly mean values, we selected monthly means of precipitation for 268 Norwegian stations through the years 1931–60 as our data sample. Most of the following study is based on such data, which give satisfactory coverage for the whole country except Finnmark. In Norway, World War II operations caused long breaks in the regular observations, and broken records were excluded from our study.

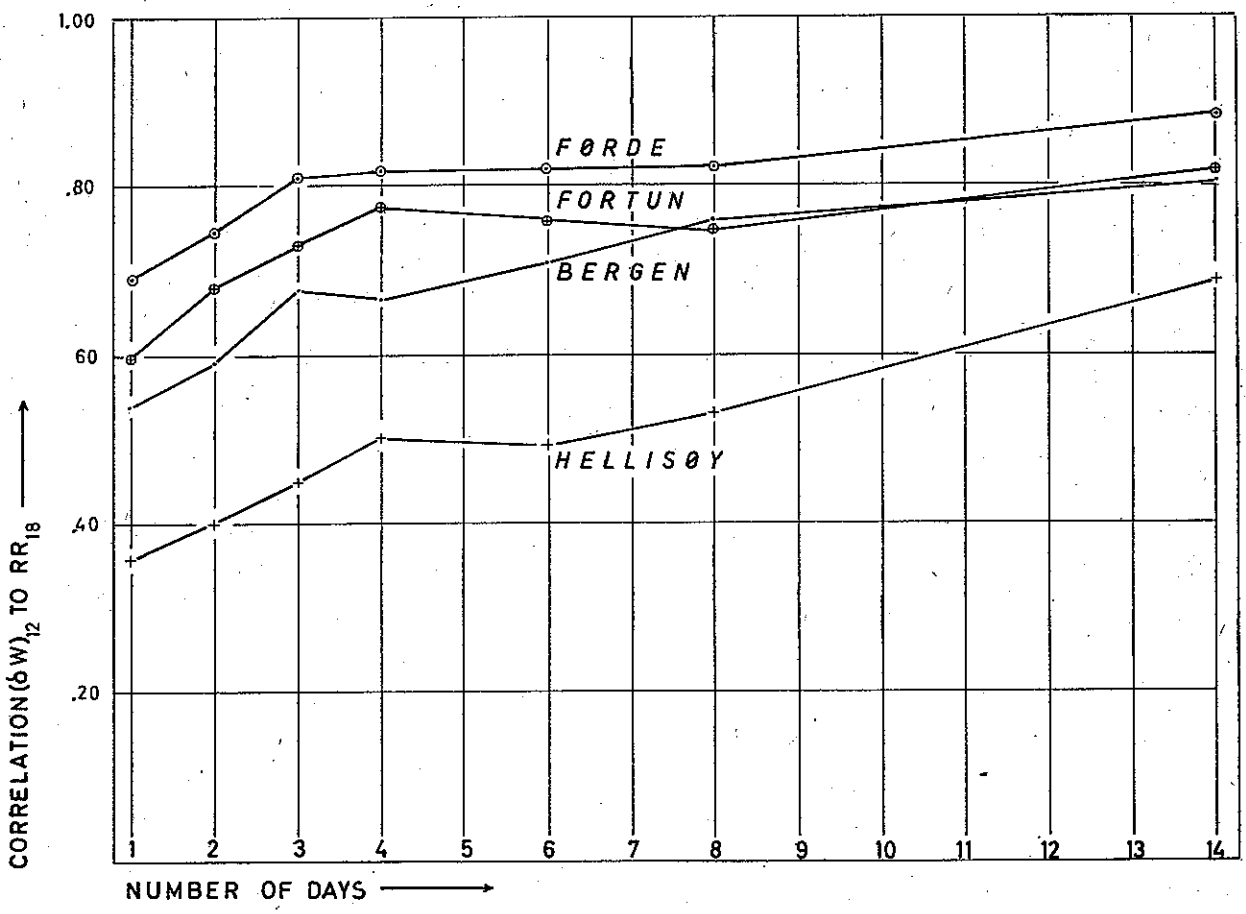


Fig. 4: Correlation between positive onshore wind, $\delta w_{12}$, and $RR_{18}$, for averages over a number of successive days.

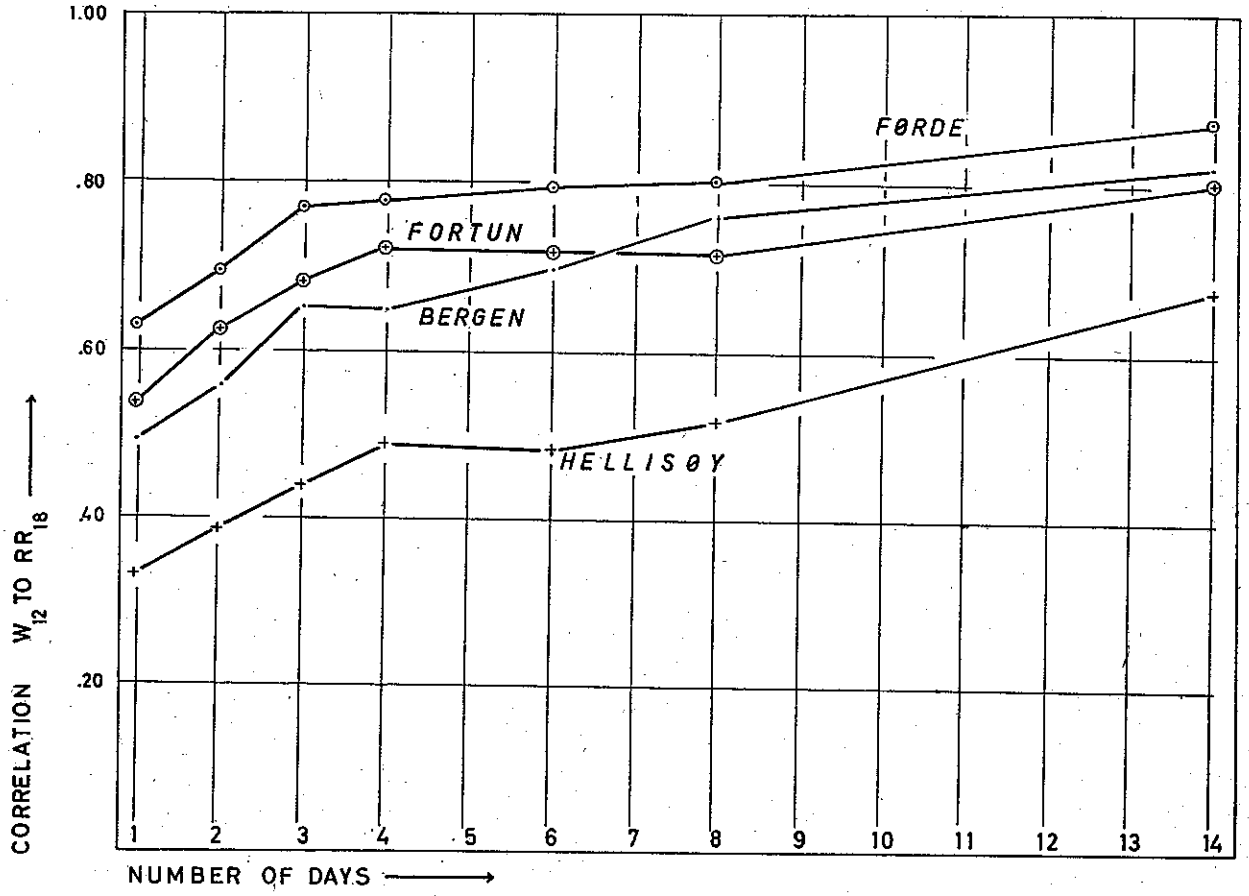


Fig. 5: Correlation between $w_{12}$ and $RR_{18}$, for averages over a number of successive days.

**3. Relations between simple flow indices and precipitation.** On the following Figures are drawn isolines for the correlation between monthly precipitation values and certain geostrophic winds. The data sample is from the period 1931–60, and the coefficient of correlation is given in units of a hundredth. Minor irregularities as well as finer structures are pointed out by plots of the respective station correlations. Fig. 6 gives the correlation analysis for the January precipitation, using the pressure difference $(p_{\text{Oksøy}}-p_{\text{Tafjord}})$ as a flow index. We notice that the correlations are almost constant in all of western Norway. A sudden drop takes place on the divide, and the correlations become negligible over eastern Norway. We also find a good correlation between our geostrophic west component and precipitation in northern Norway south of Lofoten. We may notice the drop of the correlations over the southern regions of Trøndelag. The pressure difference $(p_{\text{Tafjord}}-p_{\text{Bodø}})$ is an estimate of the onshore winds over the northern counties. In Fig. 7 we have mapped correlations between this difference and station precipitation for the month of January. The correlations are very high along the coast down to the northern parts of western Norway, and are noticeable for the remainder of this region. The transition from positive to negative correlations

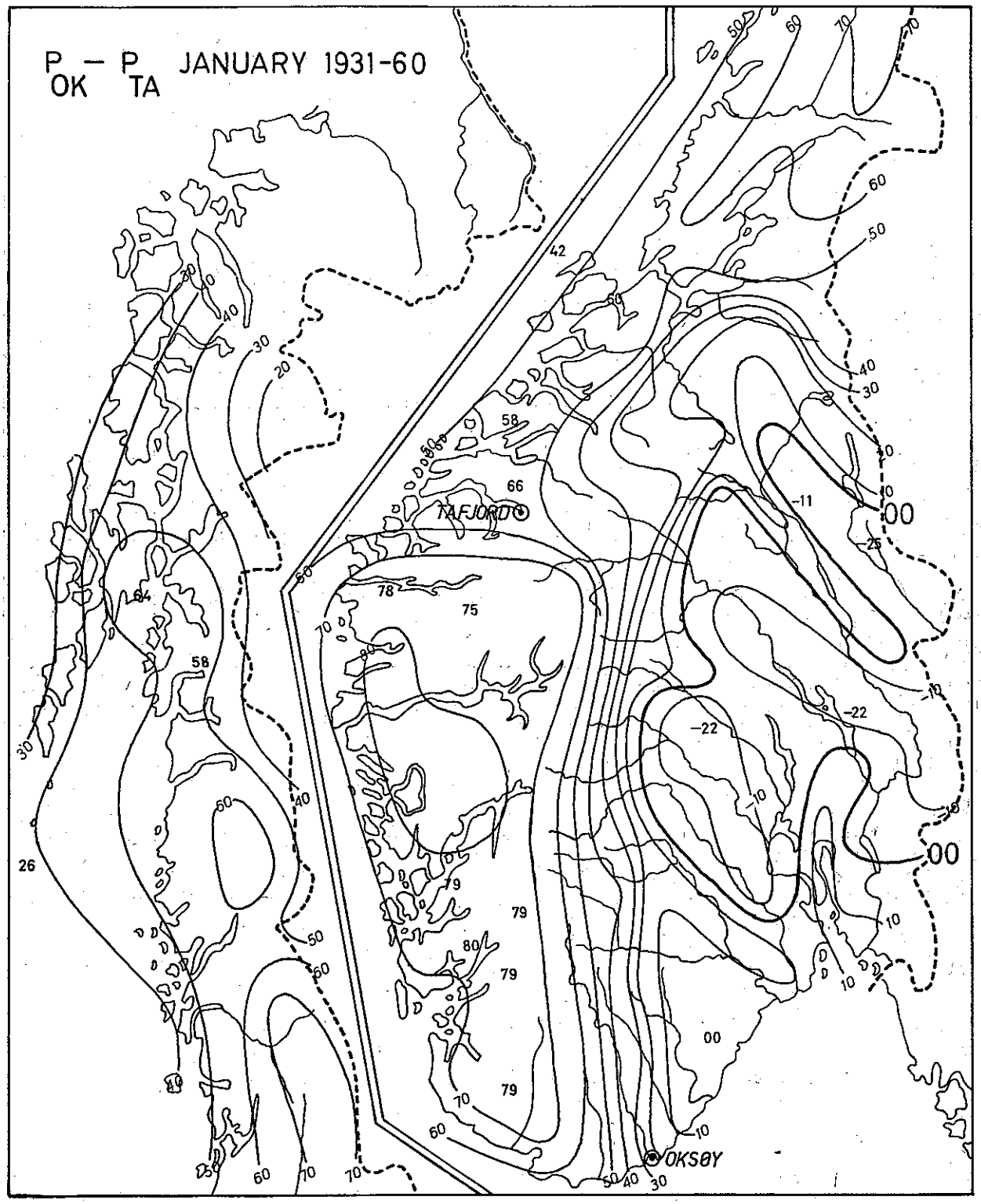


Fig. 6: Correlation between January means of ($p_{\text{Oksøy}}-p_{\text{Tafjord}}$) and precipitation.

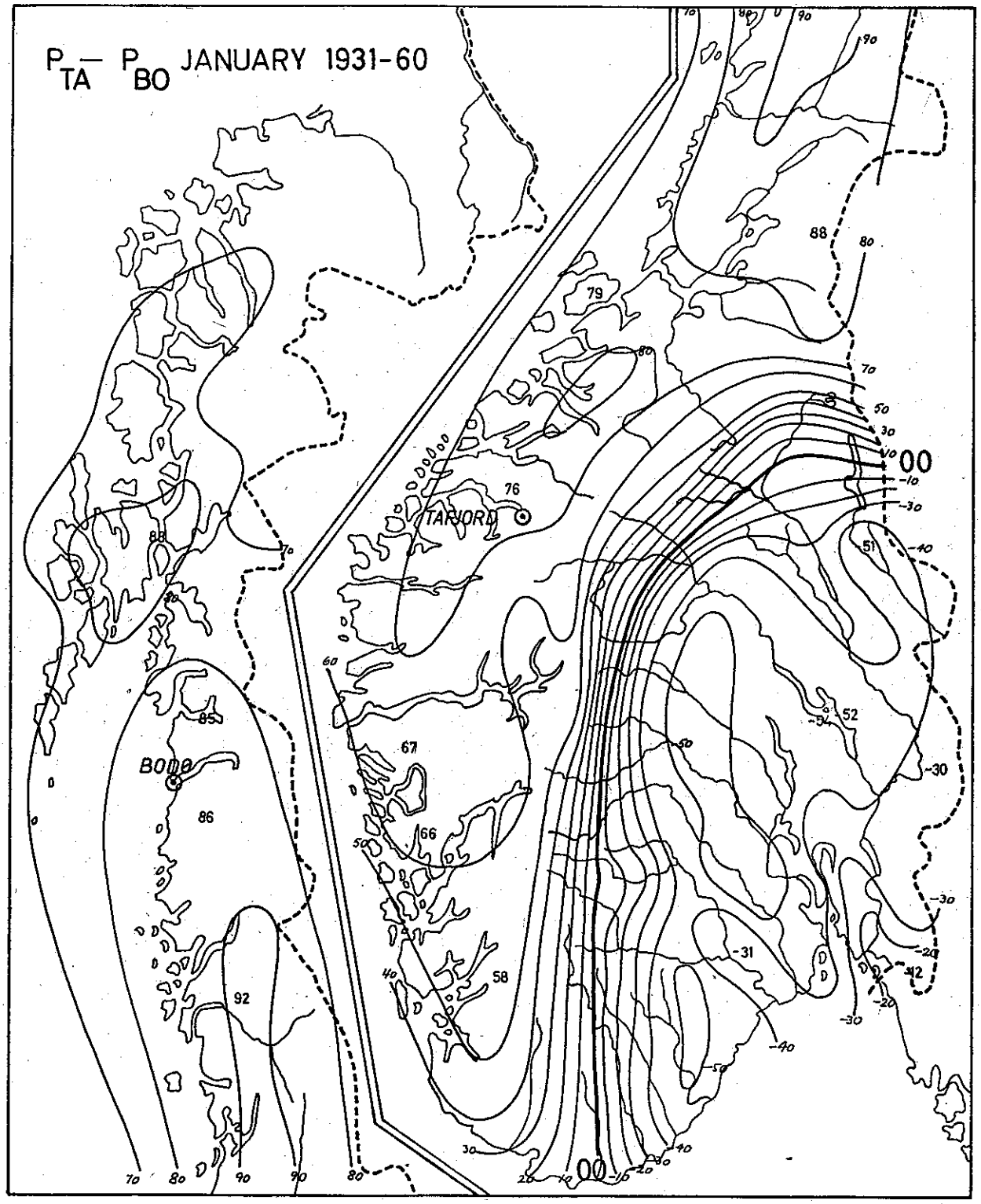


Fig. 7: Correlation between January means of $(p_{\text{Tafjord}}-p_{\text{Bodø}})$ and precipitation.

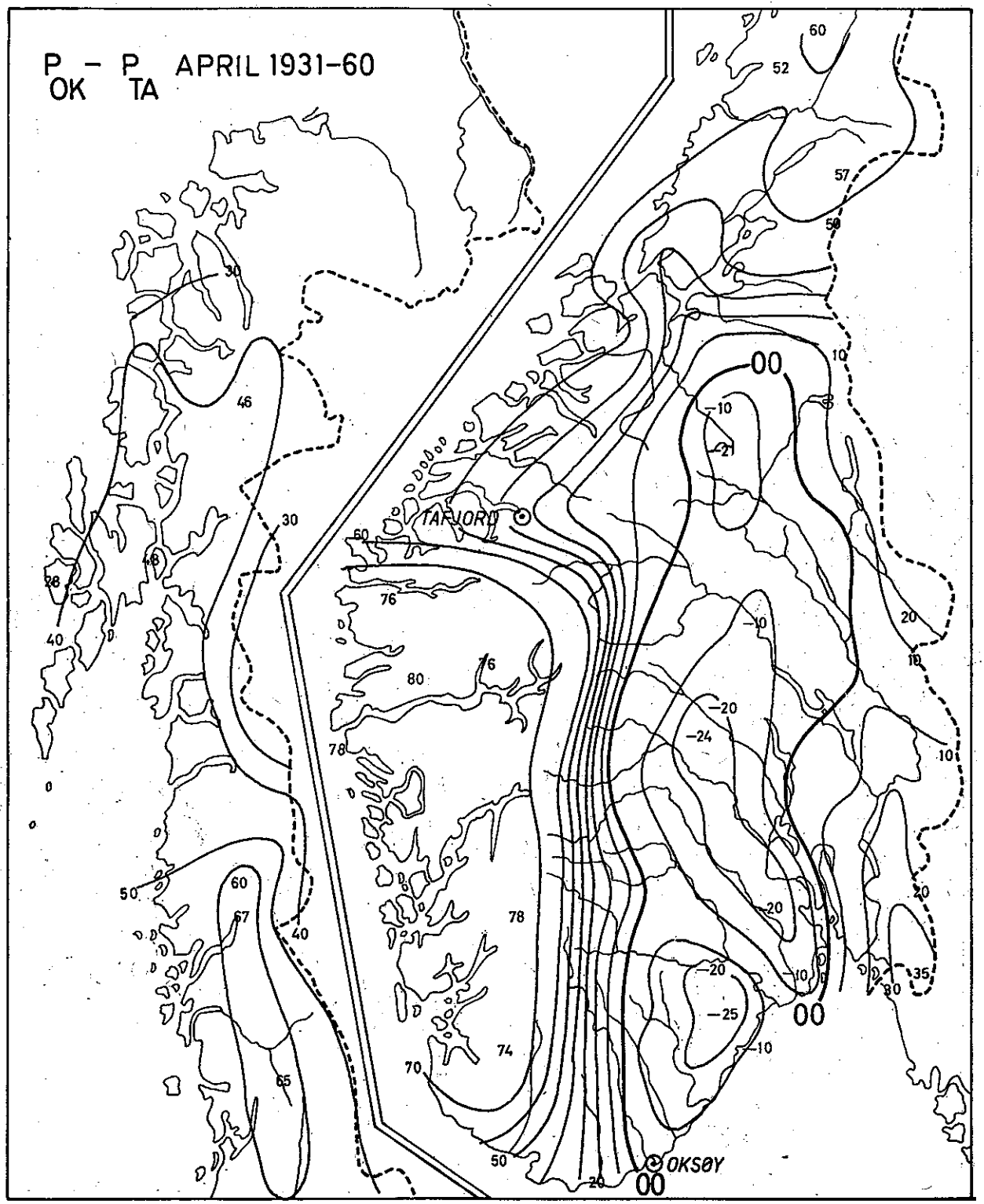


Fig. 8: Correlation between April means of ($p_{\text{Oksøy}} - p_{\text{Tafjord}}$) and precipitation.

takes place at a remarkably high rate across the divide. In Jotunheimen we observe a rate of about 20 per 10 km. The correlations drop to a level between –0.40 and –0.50 over eastern Norway, suggesting that this part of the country gets significant precipitation when exposed to southeasterly winds.

The reader may notice a certain similarity of the last two maps, and the two chosen pressure differences are indeed 0.525 correlated in January. In April this correlation drops to 0.326, indicating a smaller space scale of the monthly pressure perturbations. Figs. 8 and 9 give maps analogous to the preceding ones. We notice a drop of the positive correlations, and the negative correlation field over eastern Norway strengthens somewhat. October is another midseason month with a fairly small space scale, our geostrophic components now being 0.219 correlated. The reduced space scale is well illustrated on Fig. 10 by the rapid change of correlations in the Bodø region when heading north. A similar change is also found in September. The rain shadow over southern parts of Trøndelag is well described by the correlation field. Besides these features we find many similarities to the corresponding January map in Fig. 6. In the same manner we find good correspondence between the maps of Fig. 7 and Fig. 11, with the exception of the now much weaker correlations over western Norway. The synopticians may notice the secondary minimum over the interior parts of the Trondheimsfjord.

In July the pressure differences become –0.124 correlated. A high fraction of the local precipitation is now given by local convection, which may be released through a combination of low static stability and surface heating. But there is still a significant correlation between precipitation and onshore winds, as revealed by the next two correlation maps in Figs. 12 and 13. The correlations have dropped to about 0.70 in the regions of maximum response.

The recorded precipitation over eastern Norway has a significant negative correlation to the sea-level pressure. Figs. 14 through 17 show that $p_{\text{Oksøy}}$ is negatively correlated with precipitation for all midseason months. The numerical value of this correlation is quite stable over the year. Of interest also is the rapid change of the correlation field near Bodø in October, as given on Fig. 16. In the comments to Fig. 10 we tried to explain this finding.

**4. Annual variation of precipitation in Norway.** Strong westerly winds prevail over Norway from October through March, and the western and northern counties get most of their precipitation during this period of frequent onshore winds, see Figs. 18 and 19. Eastern Norway is well sheltered behind the divide, and the precipitation is low, especially in late winter, confer Fig. 20. The westerlies are rather weak in the summer. The static stability is low over the interior regions because of the strong heating of the land masses. The convective precipitation becomes predominant and causes a pronounced summer maximum over the interior of eastern Norway (Fig. 20) and the interior of Finnmark. Over the interior of Trøndelag this summer maximum is only slightly higher than the orographic winter maximum (with a well-defined minimum

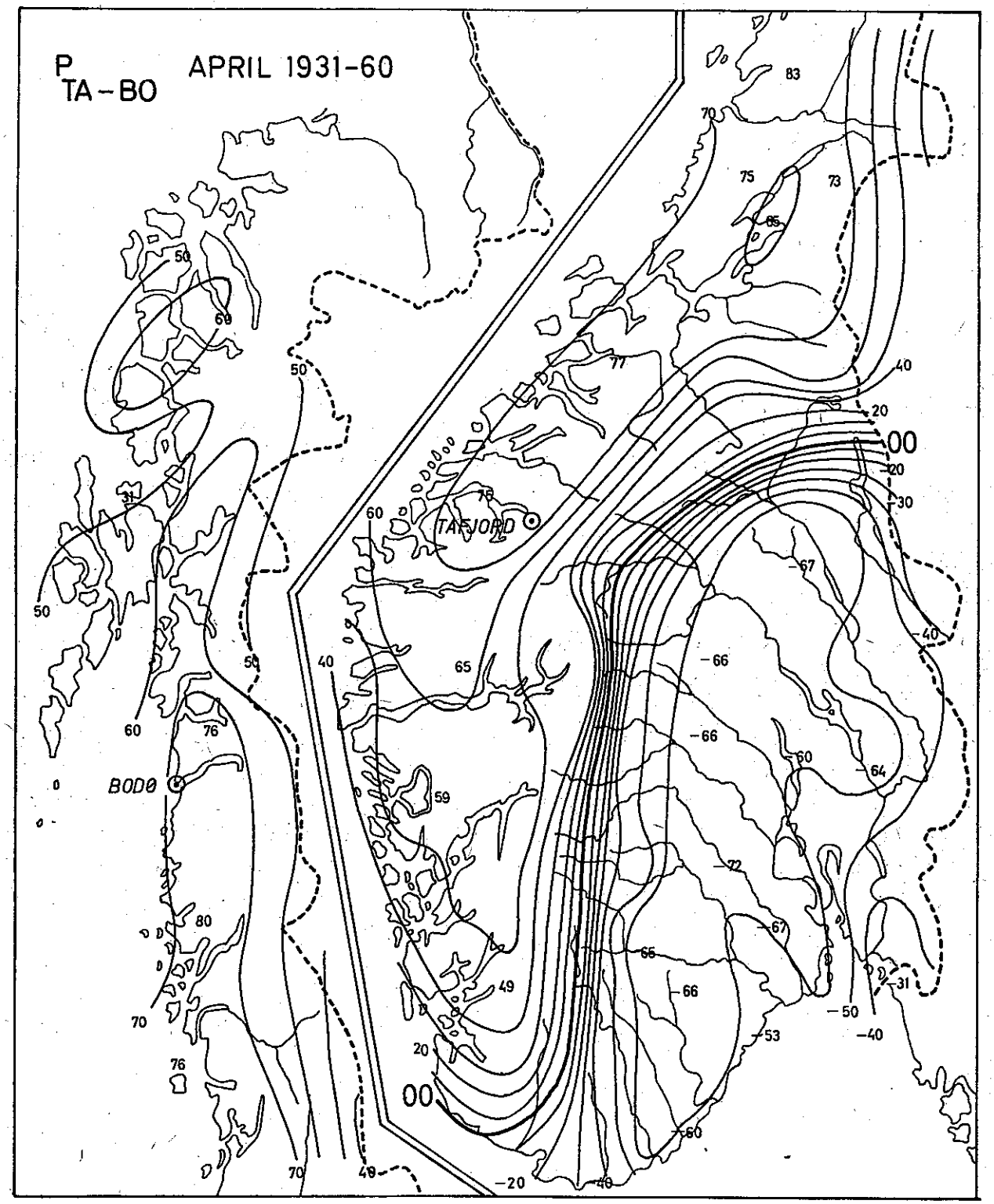


Fig. 9: Correlation between April means of ($p_{\text{Tafjord}} - p_{\text{Bodø}}$) and precipitation.

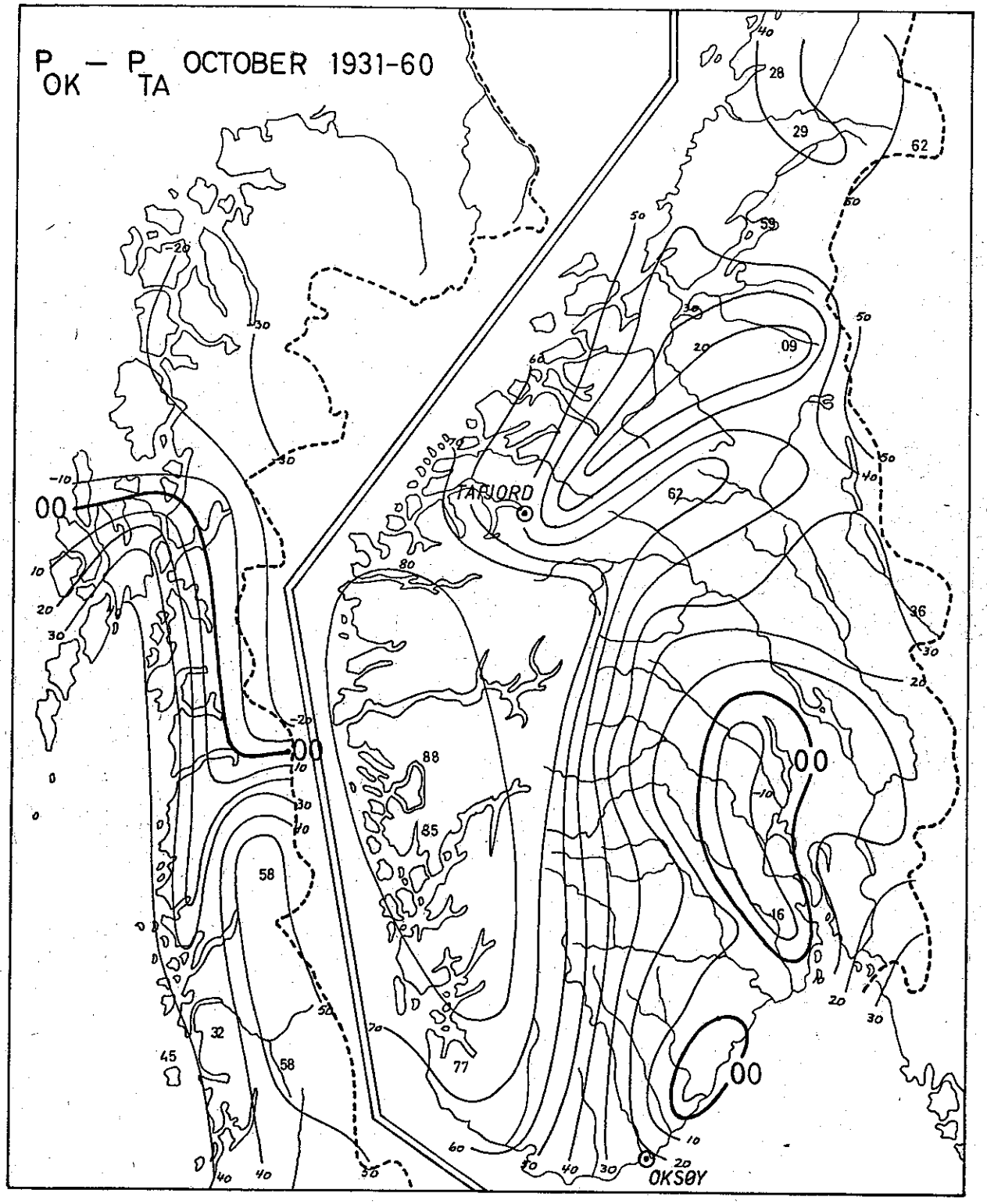


Fig. 10: Correlation between October means of ($p_{\text{Oksøy}} - p_{\text{Tafjord}}$) and precipitation.

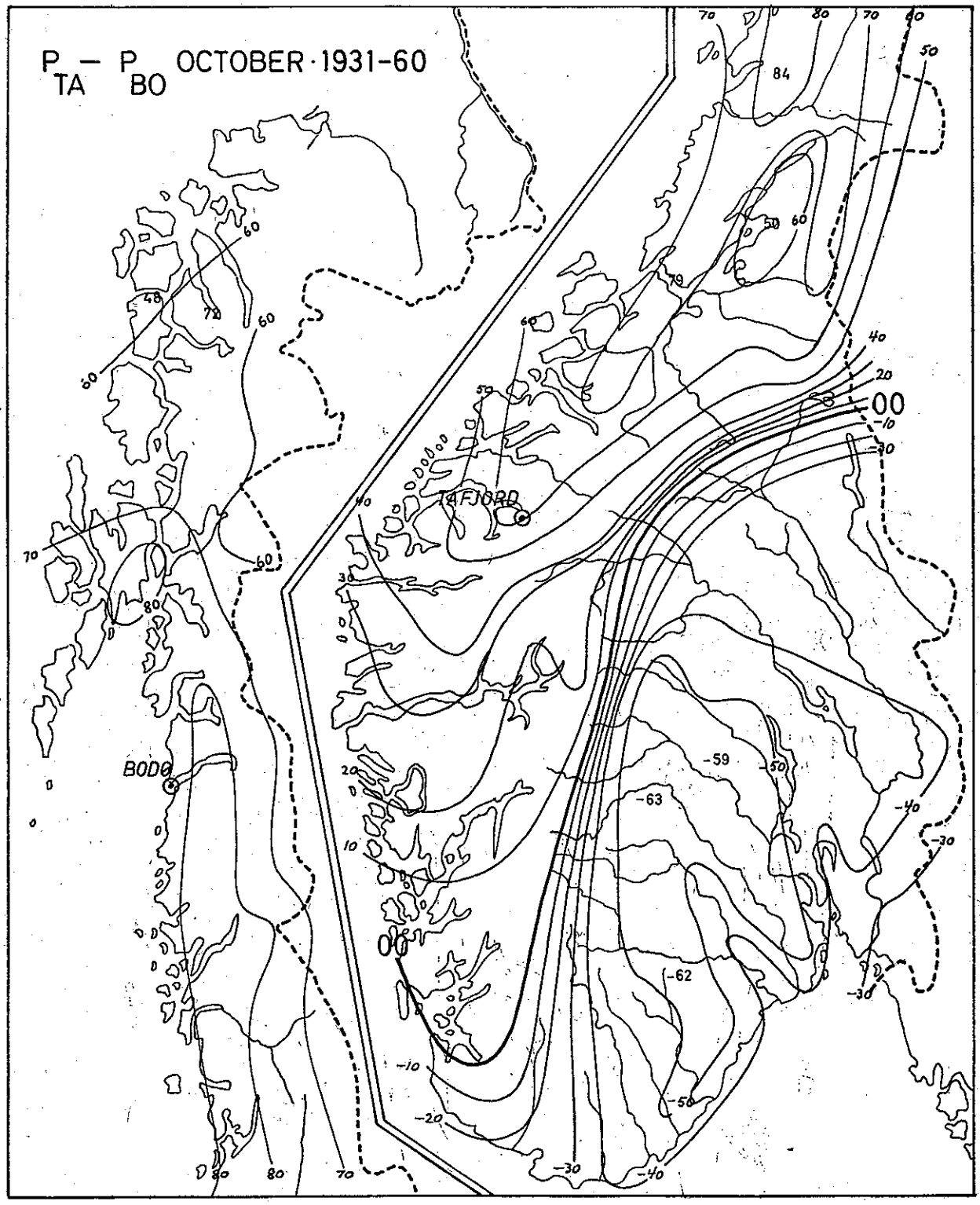


Fig. 11: Correlation between October means of ($p_{\text{Tafjord}}-p_{\text{Bodø}}$) and precipitation.

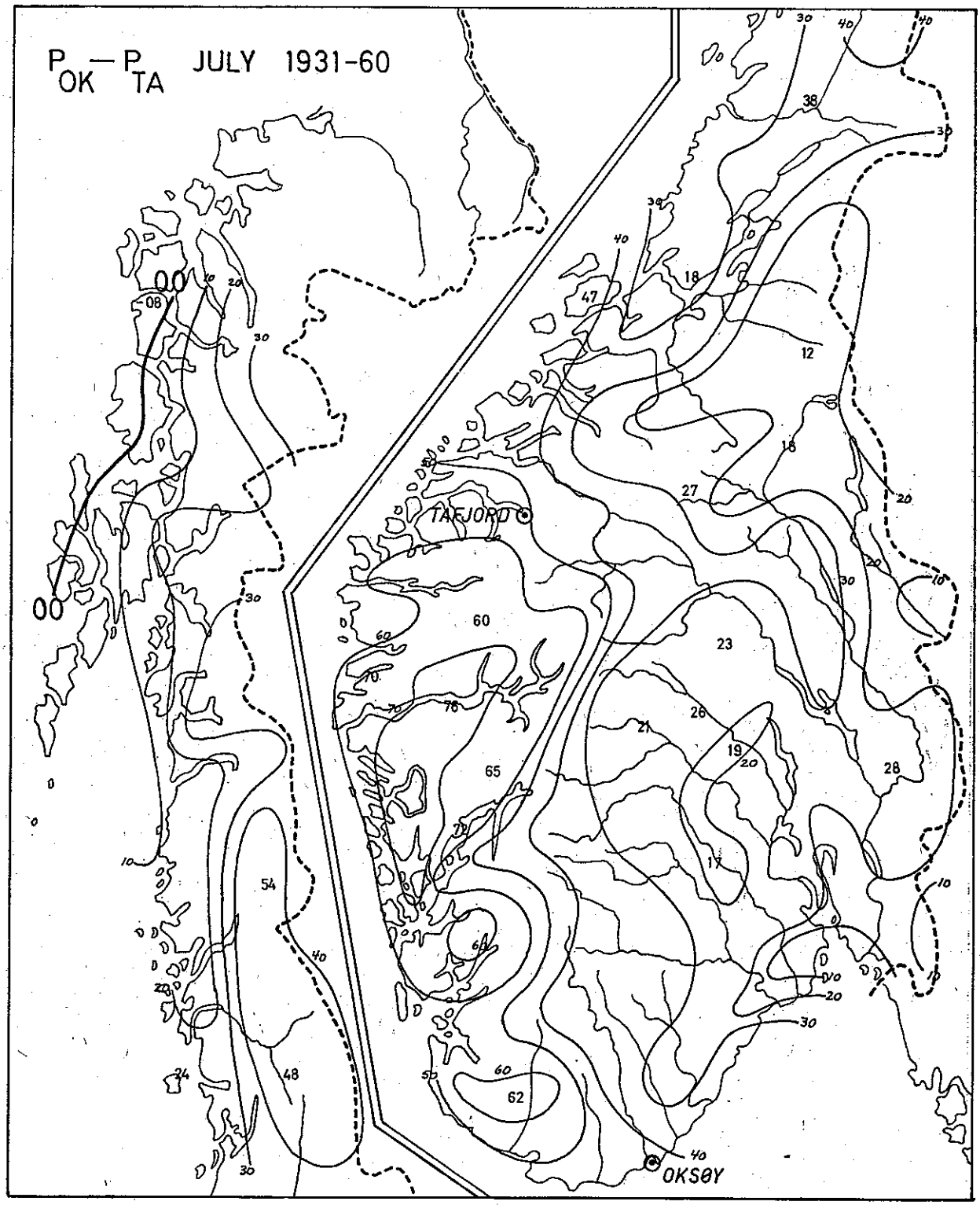


Fig. 12: Correlation between July means of ($p_{\text{Oksøy}}-p_{\text{Tafjord}}$) and rainfall.

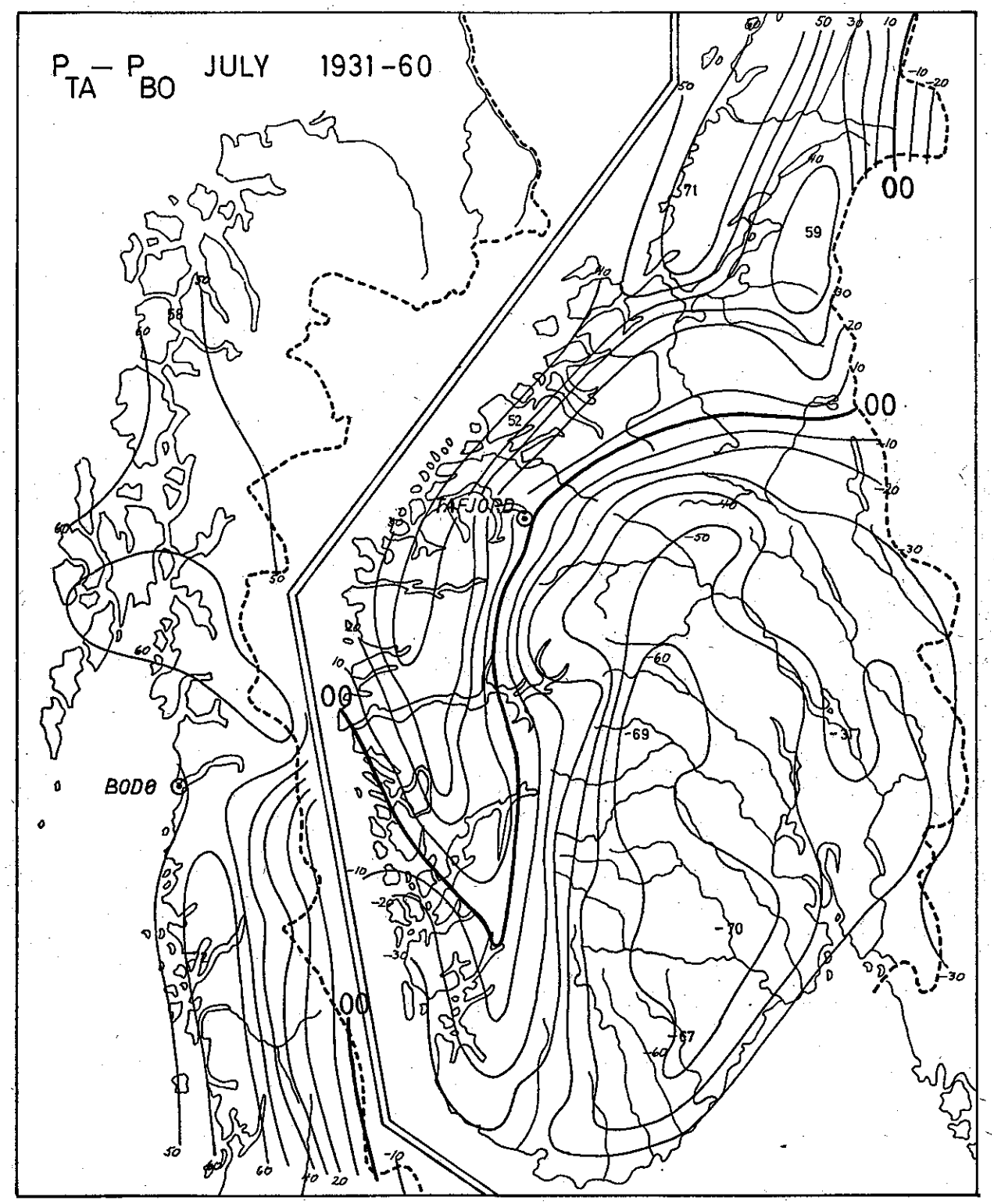


Fig. 13: Correlation between July means of ($p_{\text{Tafjord}}$–$p_{\text{Bodø}}$) and rainfall.

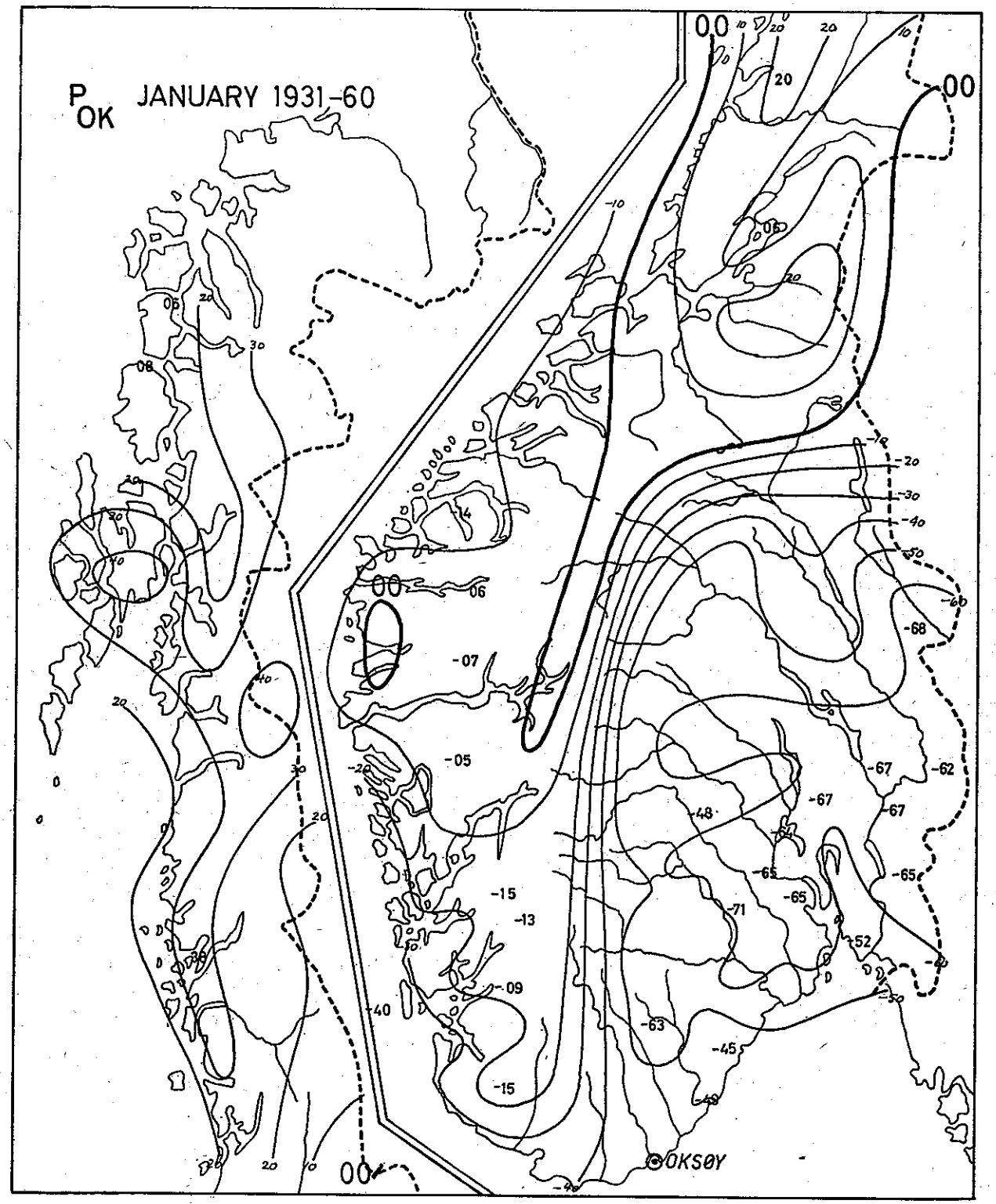


Fig. 14: Correlation between January means of $p_{\text{Oksøy}}$ and precipitation.

in late spring or early summer), see Fig. 21. Along the coast the sea is rather cold in early summer because of its high heat capacity, and, therefore, it stabilizes the air. As onshore winds are also both weak and infrequent, we observe a pronounced minimum all along the Norwegian coast this time of the year (Figs. 18 and 19).

We performed a harmonic analysis of the 12 × 30 observations using the annual sine and cosine (suffices 1 and 2), as well as the semiannual harmonics (suffices 3 and 4), in order to approximate the apparent annual variation. The square of the multiple correlation, $R^2$, then gives an estimate of how well this analytically derived curve fits an individual year. $R^2_{1.2}$ refers to the annual harmonics, which, according to Figs. 18, 19, and 20, explain 20 to 30 per cent of the total variance for the chosen stations. These correlations are high enough to give us some confidence when using the annual harmonics as an estimate of the precipitation in a given year. We also feel some security in stating that our sample of 30 years may give us the approximate real annual variation at the given locations. On Rindal in Trøndelag, however (see Fig. 21), only 9 per cent is explained by using both annual and semiannual harmonics. The fully drawn curve hardly gives a good estimate of the normal curve, nor a satisfactory estimate of a given year. Open circles in Fig. 21 with monthly normals for the preceding 30-year period illustrate the mentioned uncertainties.

The next four maps, Figs. 22 through 25, show the 30-year means of the midseason months. The main features agree well with our discussion above, but the reader should also notice the extremely low precipitation in the northern valleys of eastern Norway during the months of January and April. The October values are noticeably higher than the April values. The onshore wind is stronger in October, and we find greater variances of the wind components. The humidity content is almost 30 per cent higher in October according to the climatological tables by BIRKELAND (1944). FROGNER (1948) shows that the sea west of Norway is about 5°C warmer in October, and this difference agrees well with that of the vapour content if we assume that the air has almost the same temperature as the sea, and if the relative humidity is close to some standard value.

It might be tempting to extend our isolines out to the open sea. The coastal gradients are so strong that we may wind up with a very low precipitation at sea. But as we do not have much data to support such an extension, we have tried to be conservative when drawing the maps. Scatter diagrams for precipitation versus onshore wind reveal that the orography is significant even on the outer island stations. Fig. 26 relates precipitation on Sula with the onshore component $(p_{\text{Tafjord}} - p_{\text{Bodø}})$. For offshore winds the January values are generally low. In this connection we should like to refer to two papers by SKAAR (1955, 1965) giving extremely low annual precipitation amounts at station 'M' in the Norwegian Sea. Most estimates of precipitation on a hemispherical scale may therefore be strongly biased, as there is a tendency to extend the isolines from one orographically influenced coastal zone to another one also having orographical influences.

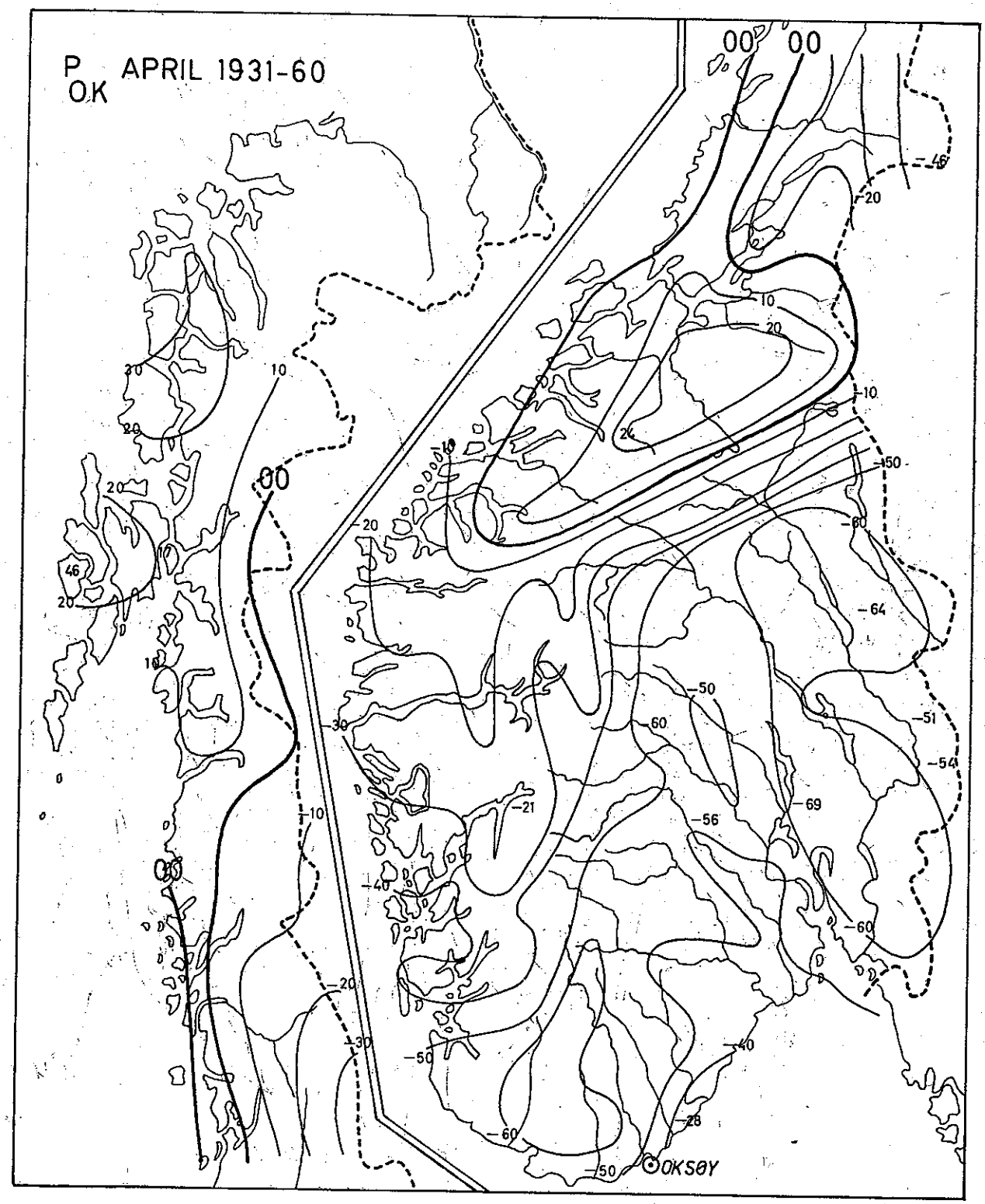


Fig. 15: Correlation between April means of $p_{\text{Oksøy}}$ and precipitation.

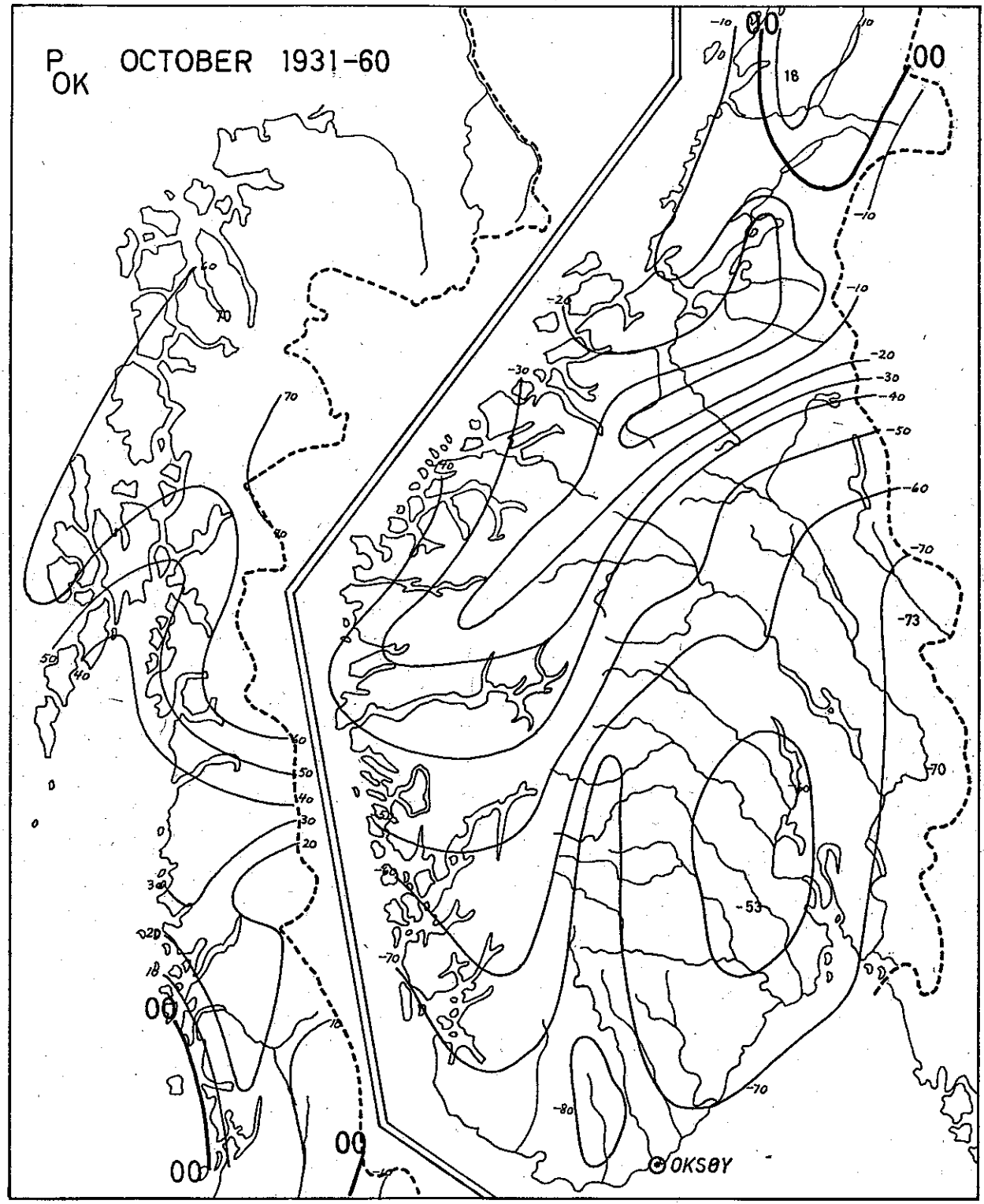


Fig. 16: Correlation between October means of $p_{\text{Oksøy}}$ and precipitation.

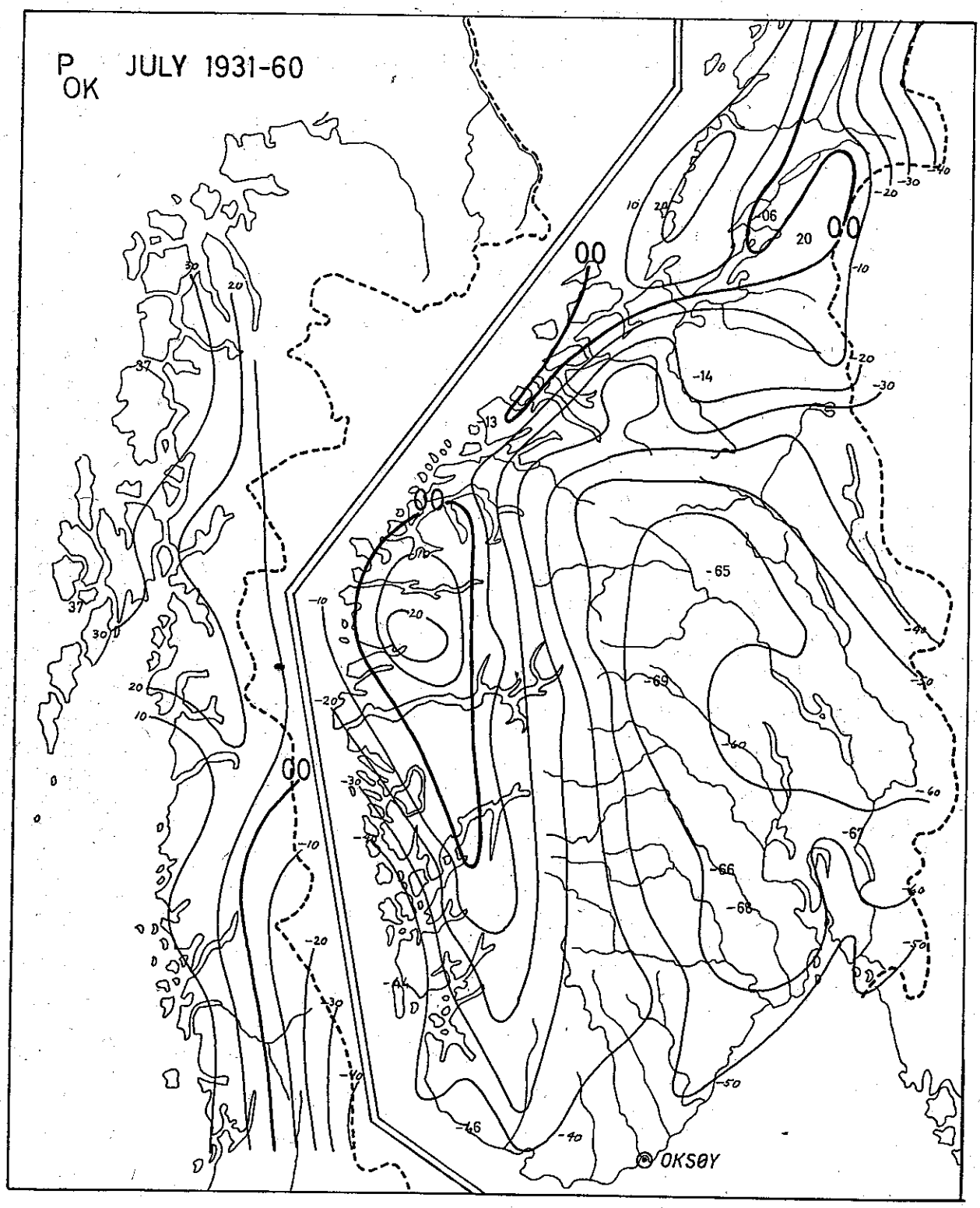


Fig. 17: Correlation between July means of $p_{\text{Oksøy}}$ and precipitation.

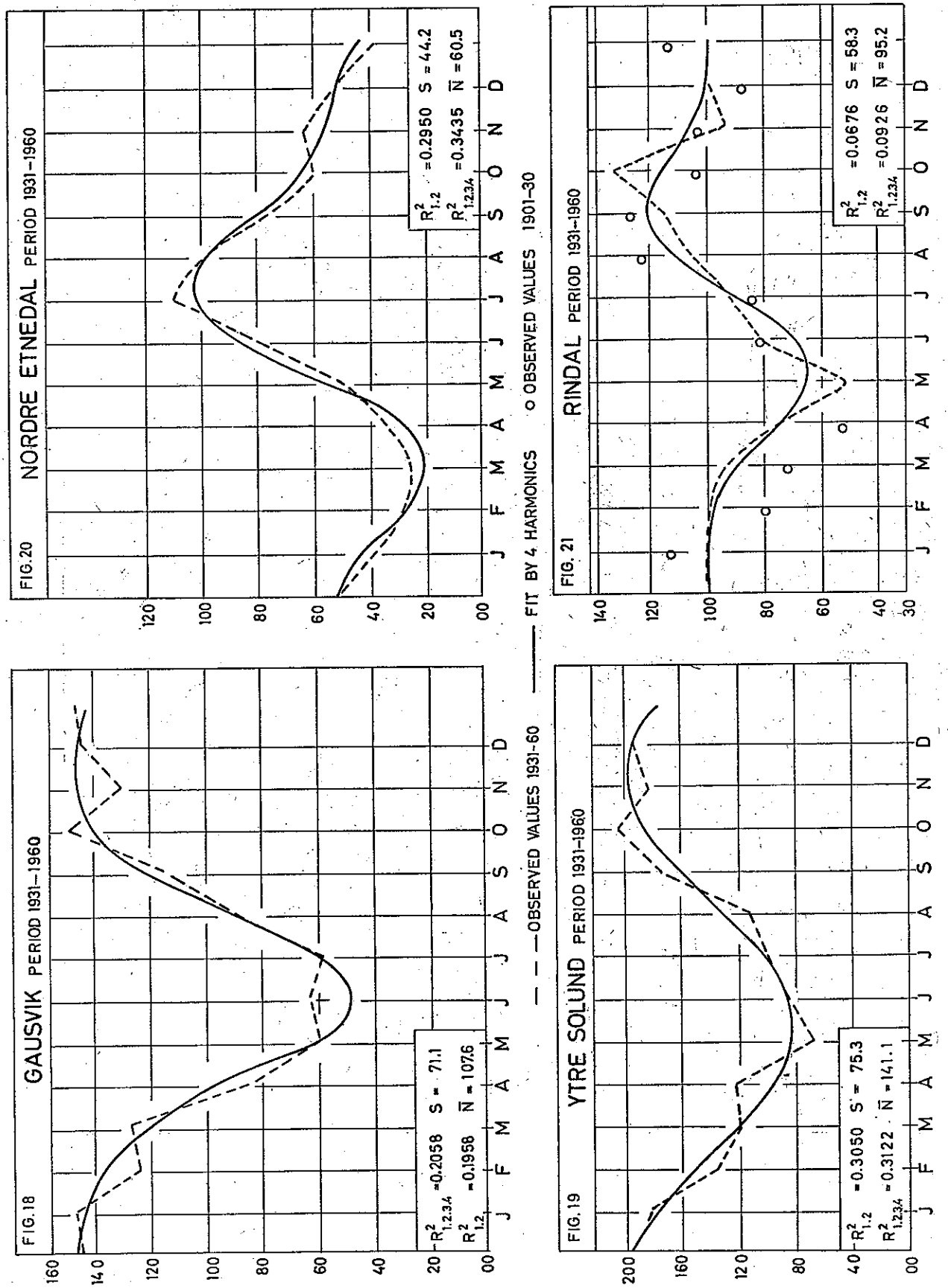


Fig. 18: Annual variation of precipitation at Gausvik (69° N) in northern Norway.
Fig. 19: Annual variation of precipitation at Solund (61° N) in western Norway.
Fig. 20: Annual variation of precipitation at Nord Etnedal (61° N) in eastern Norway.
Fig. 21: Annual variation of precipitation at Rindal (63° N) in Trøndelag.

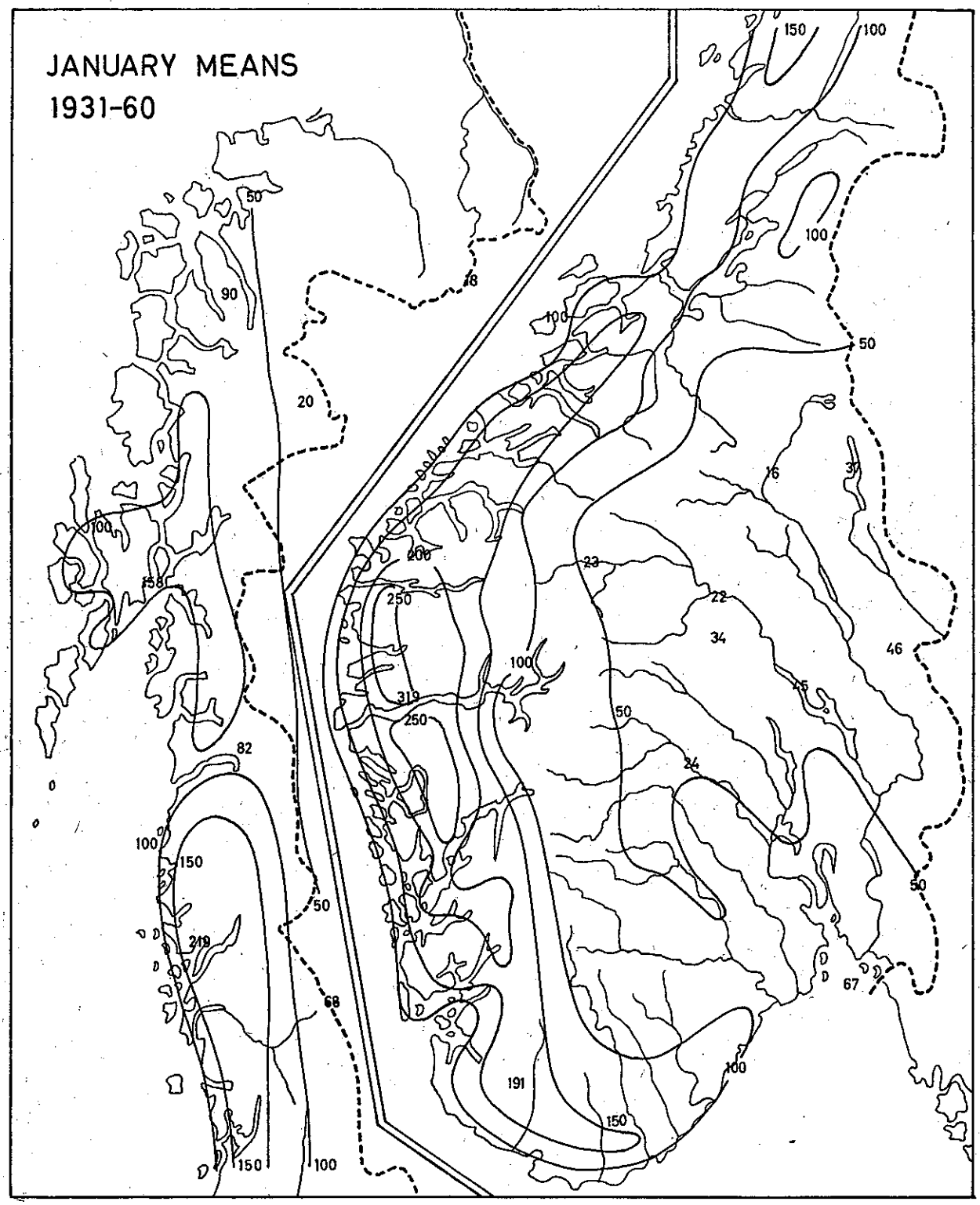


Fig. 22: Average January precipitation in the period 1931–60.

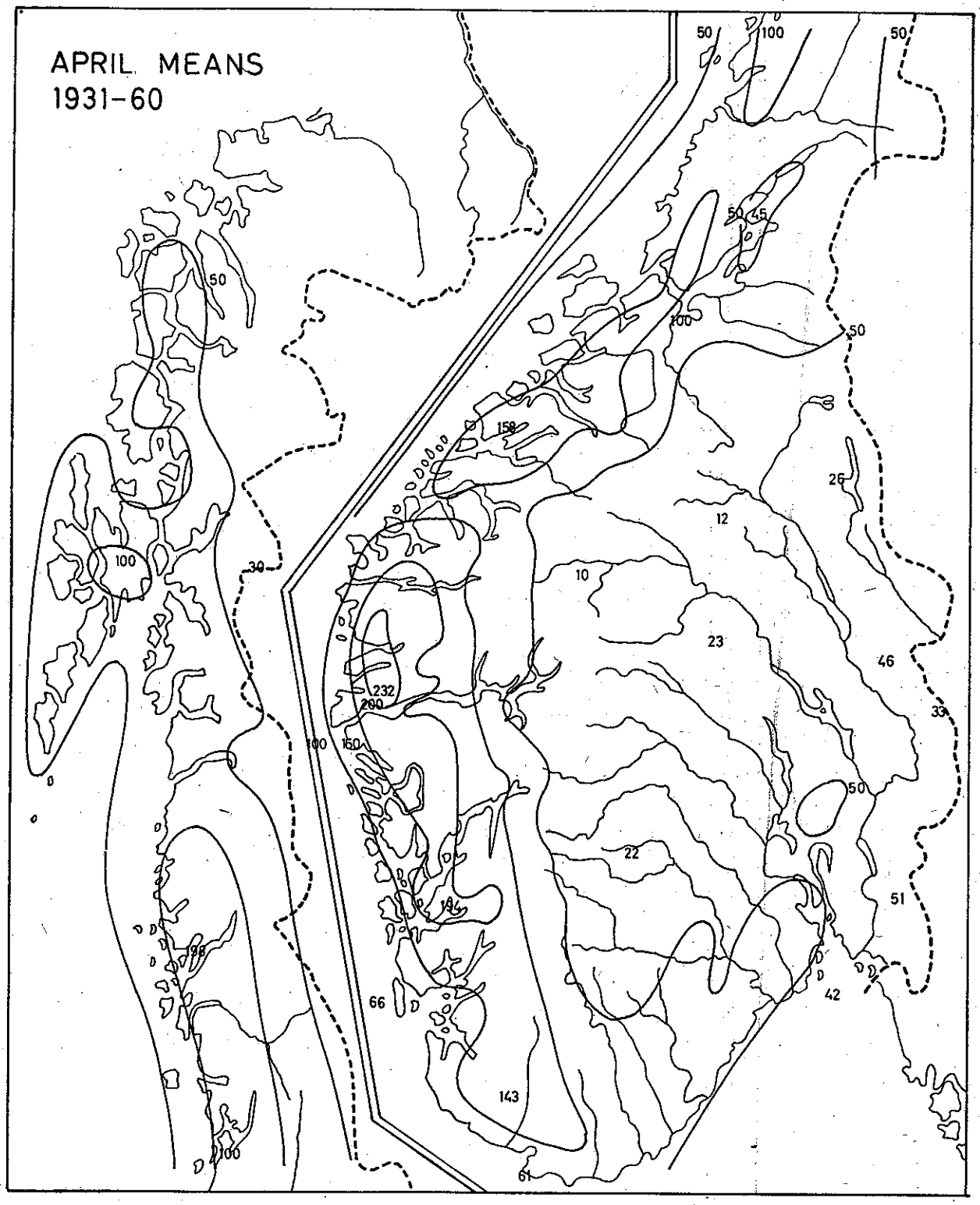


Fig. 23: Average April precipitation in the period 1931–60.

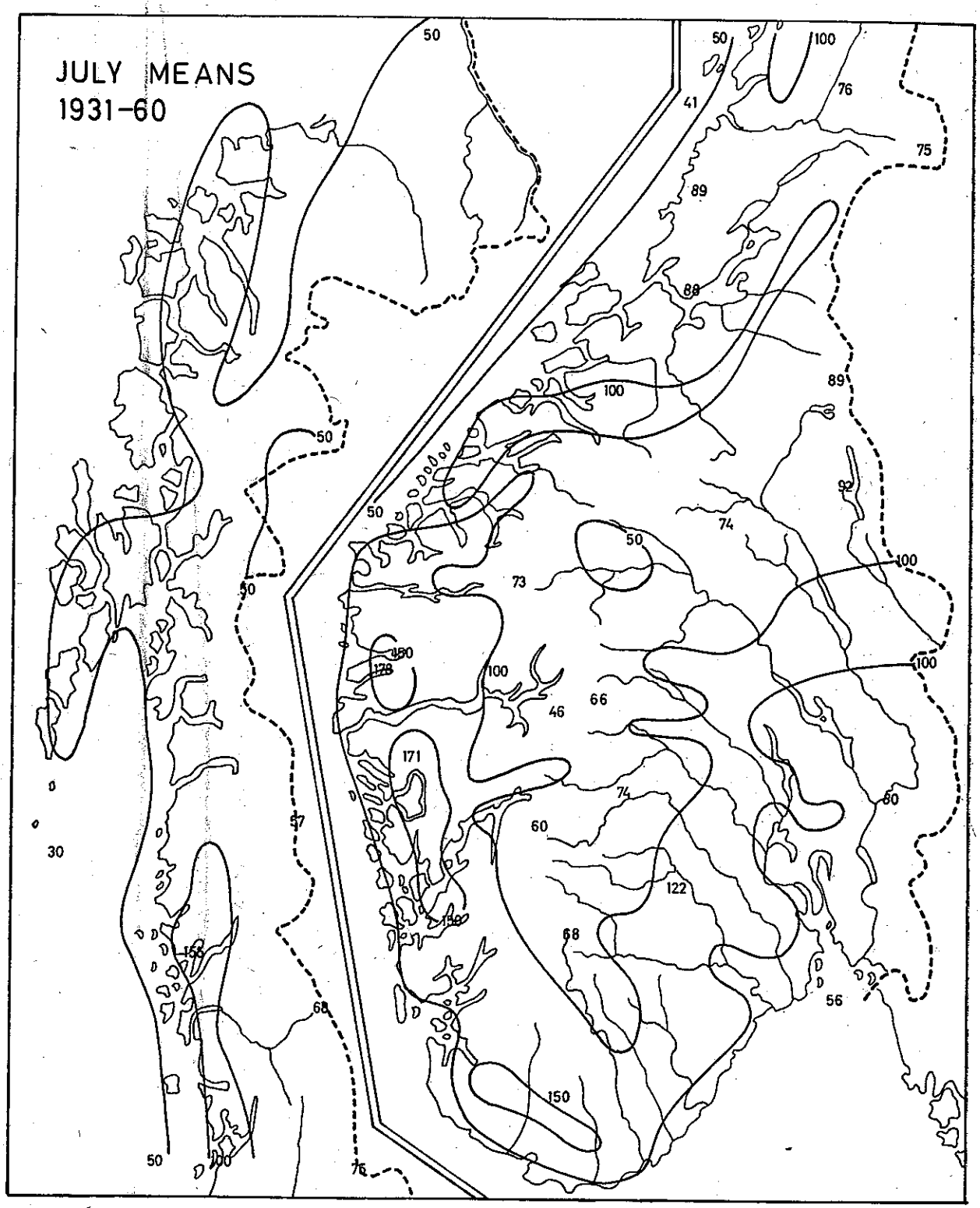


Fig. 24: Average July precipitation in the period 1931–60.

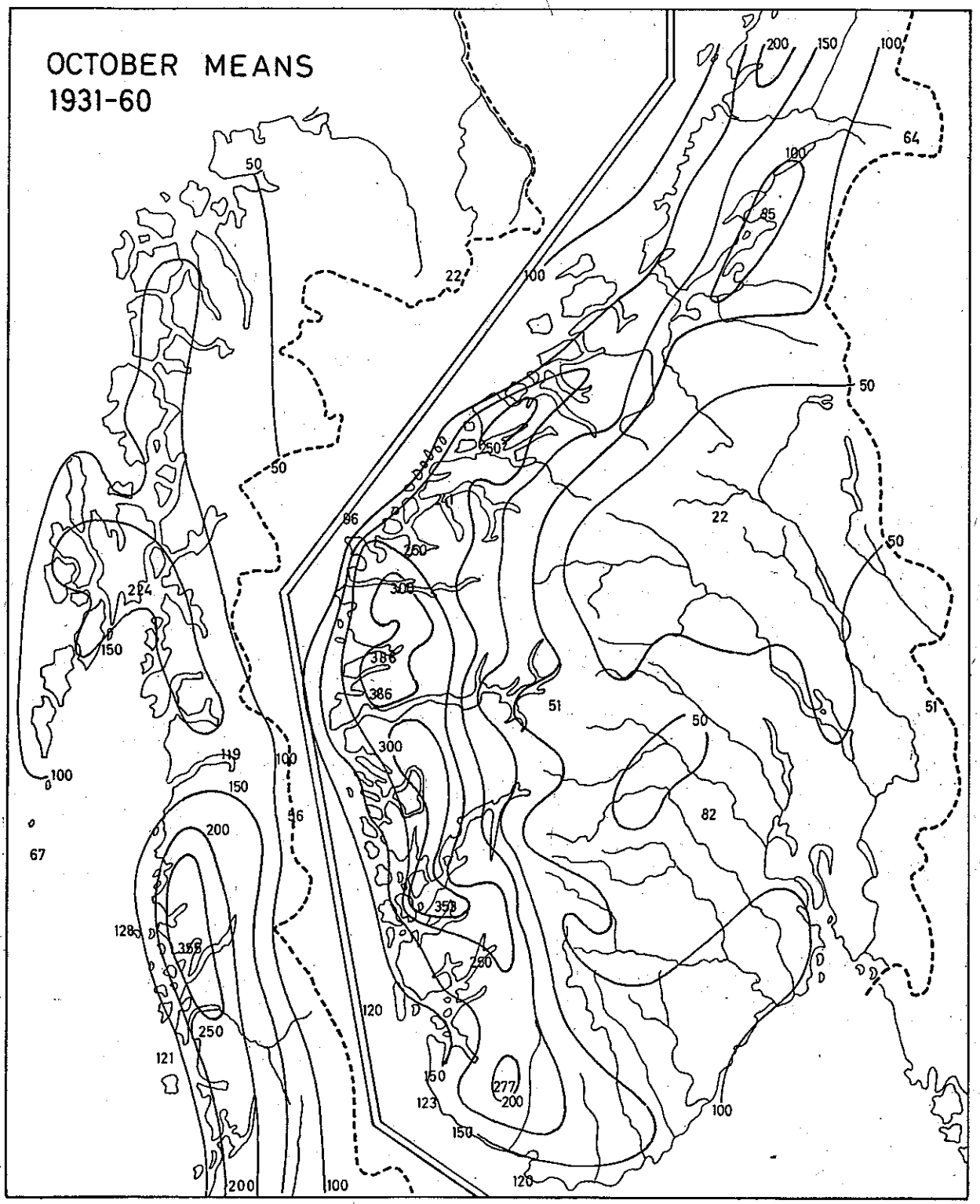


Fig. 25: Average October precipitation in the period 1931–60.

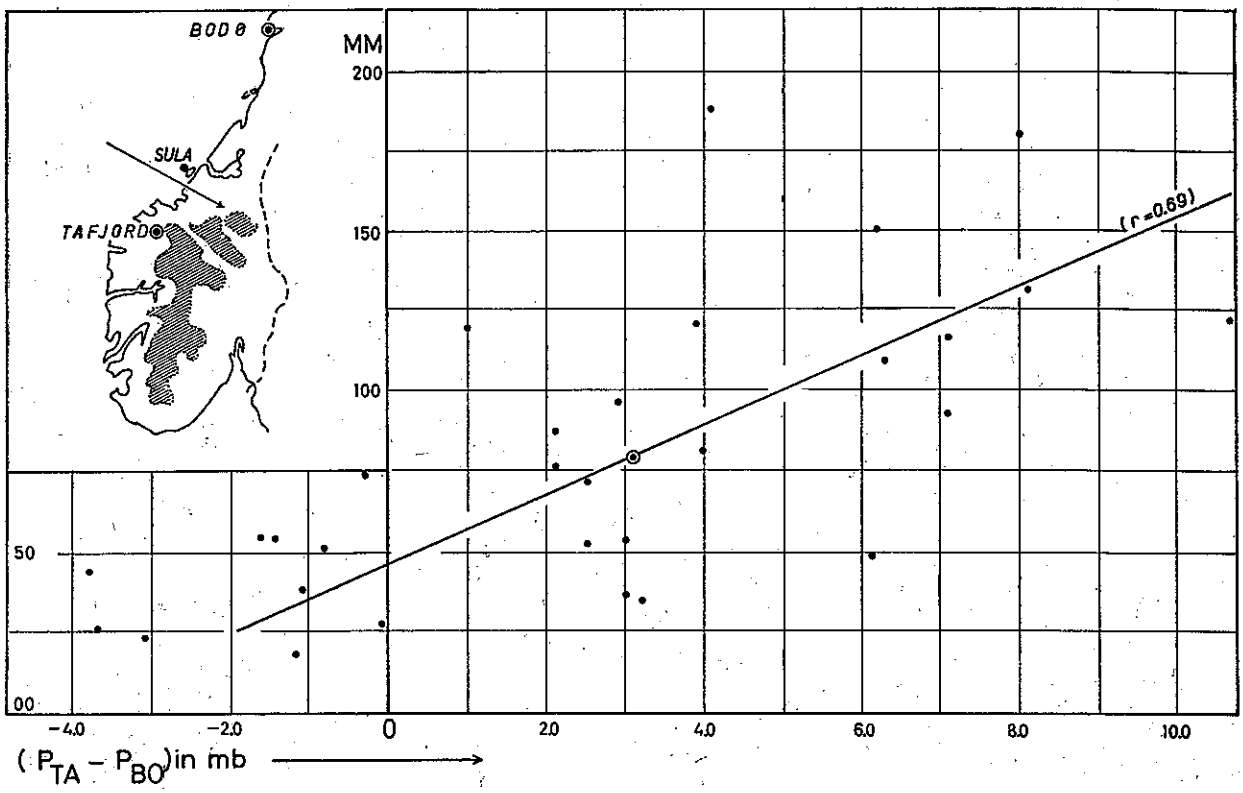


Fig. 26: Scatter diagram of January precipitation on Sula versus geostrophic wind measured by ($p_{\text{Tafjord}} - p_{\text{Bodø}}$).

For monthly precipitation the ratio of the standard deviation to the mean (S.D./mean) has a smoother distribution then the standard deviation alone. Annual variations of the frequency distribution will effect this ratio. Skew distributions have fairly high ratios (the frequency distribution $e^{-at}$ has a ratio of 1.00), more symmetric distributions tend to have lower ratios. As the orographic effect depends only on the onshore wind component, the resulting skew distribution should have a peak frequency for a value significantly lower than the mean. In summer the convective precipitation occurs mostly in air masses with low tropospheric temperatures, and we may expect a less asymmetric distribution of rainfall. The precipitation from fronts and eddies on a synoptic scale should also give fairly symmetric distributions, as evidenced by observations on the outer island stations.

In Fig. 27 the ratio S.D./mean is plotted in hundredths for all midseason months for a number of stations. The January ratio (upper left) as well as the April ratio (upper right) are both high in the orographic zone. On the coast the ratios are lower, as expected. The July ratio (lower left) is generally low, as the convective and cyclone precipitation are dominant. The October ratios (lower right) are also comparatively low in southern Norway, especially when compared with the April ratios. Forming the ratio S.D./mean for the pressure difference ($p_{\text{Oksøy}} - p_{\text{Tafjord}}$), we find values of

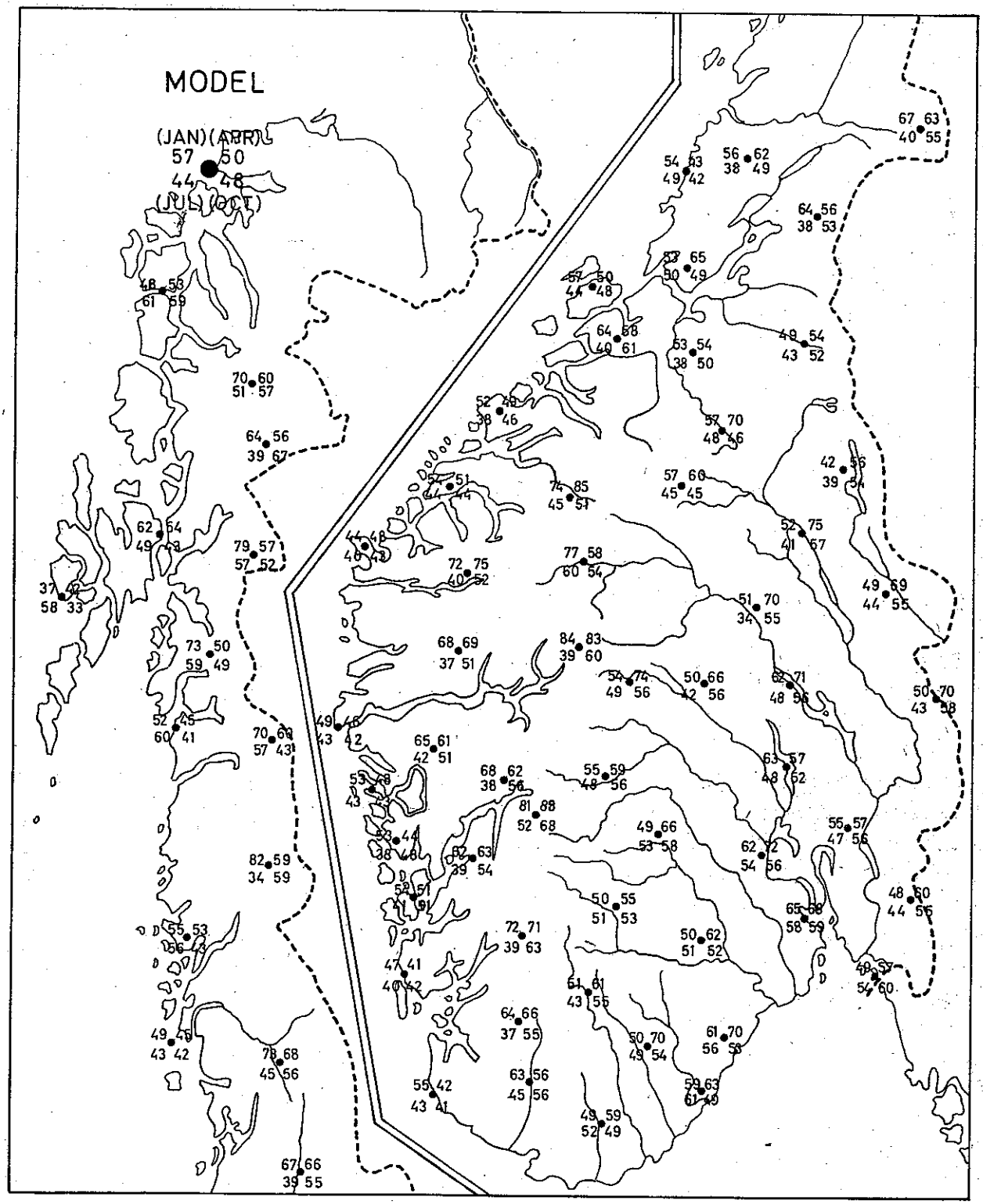


Fig. 27: Ratio standard deviation to mean in hundredths for all midseason months.

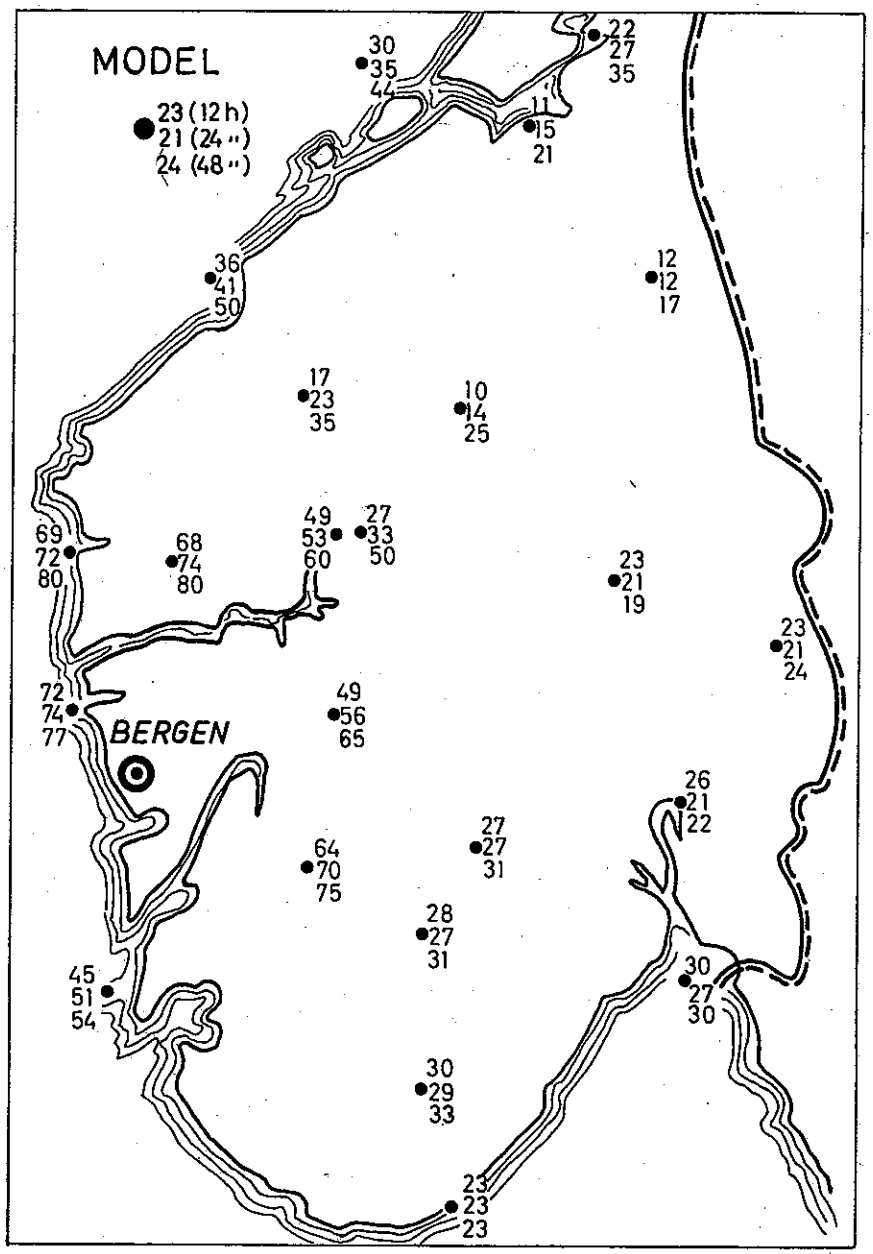


Fig. 28: Space correlation of 12-hour, 24-hour, and 48-hour precipitation with Bergen as a reference station.

1.16 in April and 0.79 in October, respectively. Blocking circulations over the eastern Atlantic and Scandinavia are also more frequent in April than in October.

**5. Space correlations of precipitation.** In Fig. 4 was demonstrated the increased correlation between precipitation and onshore wind when averaged over successive 12-hour intervals. The same increase may therefore be expected of the space correlations for precipitation records of stations situated on the same side of the highest mountain ranges. Taking, e.g., Bergen as a reference station and using January–

February data, Fig. 28 gives various coefficients of correlation in hundredths. For a few stations we have plotted three values in Fig. 28, the upper one gives the correlation for the 12-hour precipitations, the middle value correlation for 24-hour records, and the lower one correlation for 48-hours precipitation. The listed values clearly point out the expected increase of space correlations in the western region, when using precipitation records over increasing lengths of time. With monthly means, this space correlation becomes high over western Norway. By considering the extreme month of February and picking the station Haukedal in the maximum zone as a reference, we derived the remarkably high correlations in Region A of Fig. 29. The space correlations are

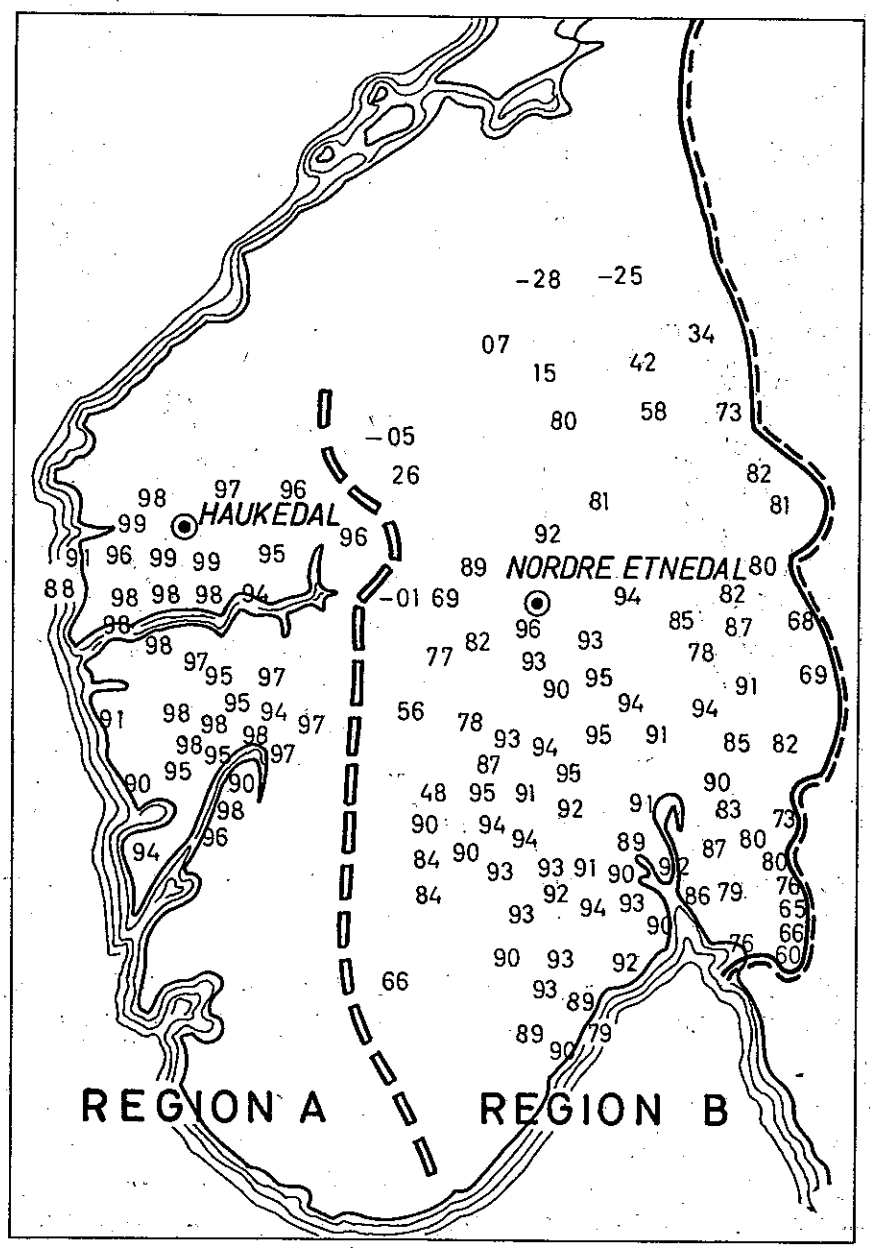


Fig. 29: Space correlations of February precipitation with Haukedal and Nordre Etnedal as reference stations.

also high over eastern Norway, as revealed by Region B, where Nordre Etnedal is picked as a reference station. Heading across the western divide the correlations suddenly drop to zero. This abrupt change must be caused by the opposite orographic exposure of the stations, as the non-orographic precipitation field should have a much larger space scale.

We finally present space correlation maps for all midseason months, and use Haukedal and Nordre Etnedal as the reference stations. Figs. 30 and 31 show the correlation fields in January. We find rather strong gradients slightly east of the divide. On the same side of the divide, however, most of the area lies inside the 0.80 isoline. In April we find similar results, but the 0.80 isolines have contracted somewhat on Figs. 32 and 33. The negative correlations are more pronounced than in January. The October space correlations have generally the same distribution, but the gradients are weaker across the divide, confer Figs. 34 and 35. In July the region of high gradients moves west of the divide and rather close to the zone of maximum mountain slope. The decreased orographic rainfall, because of light winds as well as the increased inland convection from strong surface heating, may explain the July fields of Figs. 36 and 37.

The annual variation of space correlation, using Haukedal as a reference station, agrees well with what we found when correlating precipitation with the westerly flow index $(p_{\text{Oksøy}}-p_{\text{Tafjord}})$. But the correlations are somewhat higher west of the divide. This result was anticipated, as we should have used the monthly mean of the positive onshore component $\partial w$ instead of the mean of $w$, see Figs. 4 and 5 for quantitative estimates. In this connection we should be aware that the onshore geostrophic wind is not always a good estimate of the vertically integrated onshore wind. We know also that features like fronts and lows may cross the western region and give significant precipitation which may not be accounted for by the difference $(p_{\text{Oksøy}}-p_{\text{Tafjord}})$.

**6. A more complete specification of precipitation as a function of circulation on local and continental scales.** So far we have presented a rather straightforward analysis of our data. More complex studies have been undertaken, using a general search program developed by NORDØ (1960, 1966). This program scans linear combinations of all the variables, and prints out the five best sets of two variables, the five best sets of three variables, etc. The program can, on request, introduce derived quantities as additional variables. In this manner we were able to perform a more complex analysis of our data. As a supplement to the results given in the previous sections, we shall look at an investigation relating precipitation to the temperatures and pressures of certain reference stations. In order to make the results comparable, we shall use *standardized* precipitation values $\left(\frac{\Delta RR}{S.D.}\right)$. If pressure is measured in mb and temperature in °C, we shall give the various weights in hundredths. The weights are put in brackets underneath the station dot. Above the dot we give the coefficient of multiple correlation in hundredths. Fig. 38 presents the results for the October precipitation. Along the Atlantic coast two station pressures give an optimal description of the precipitation.

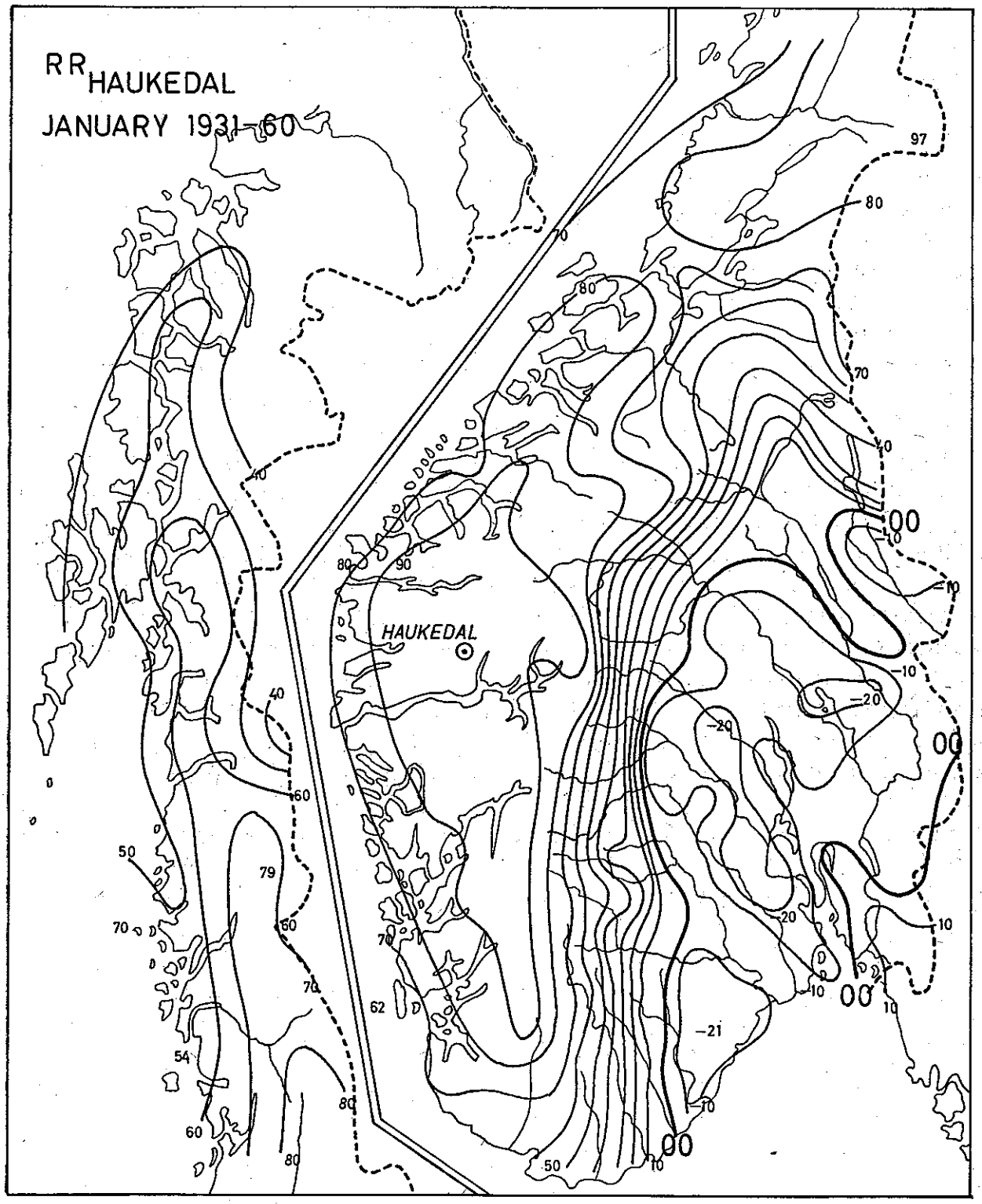


Fig. 30: Space correlation of January precipitation with Haukedal as reference station.

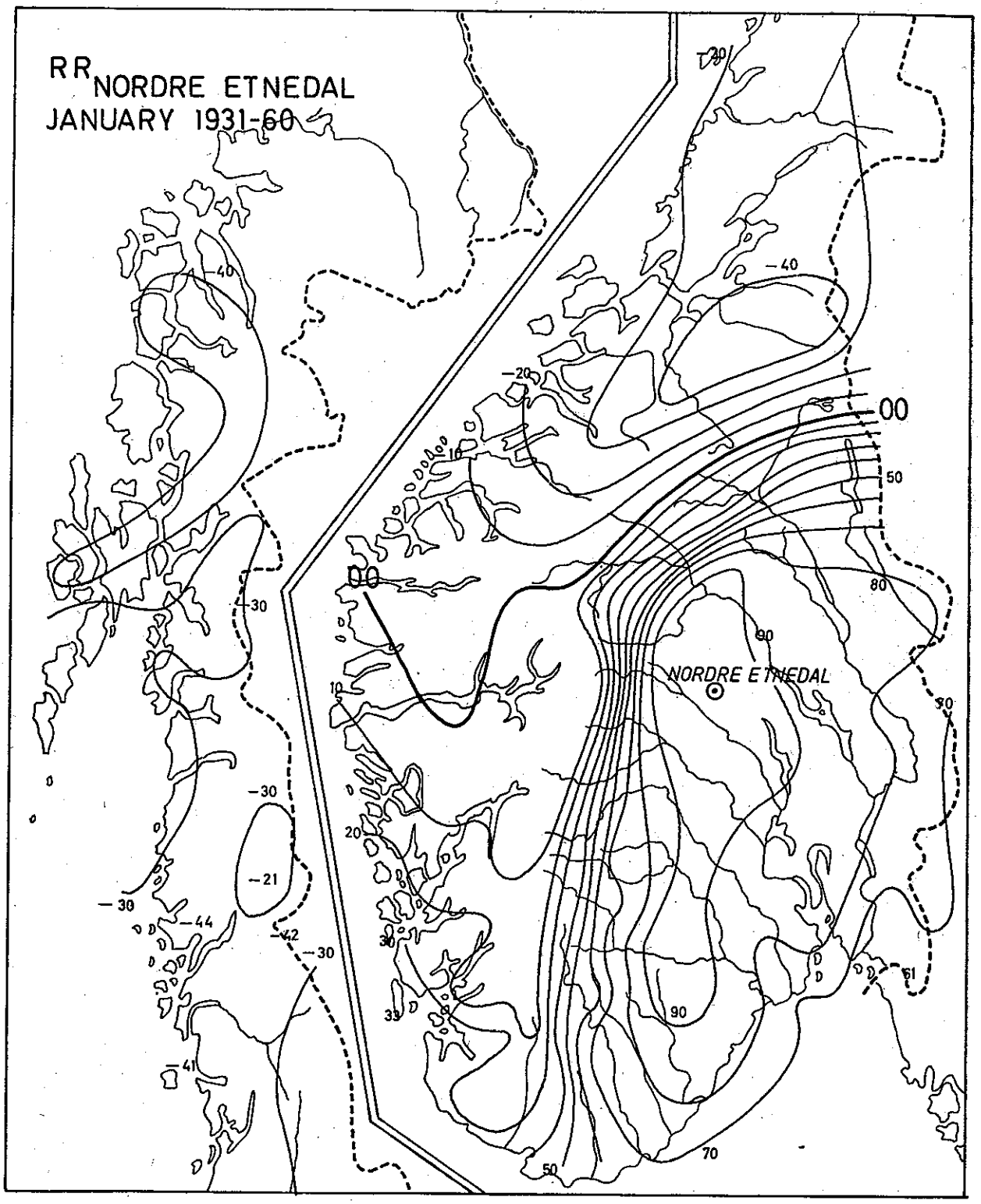


Fig. 31: Space correlation of January precipitation with Nordre Etnedal as reference station.

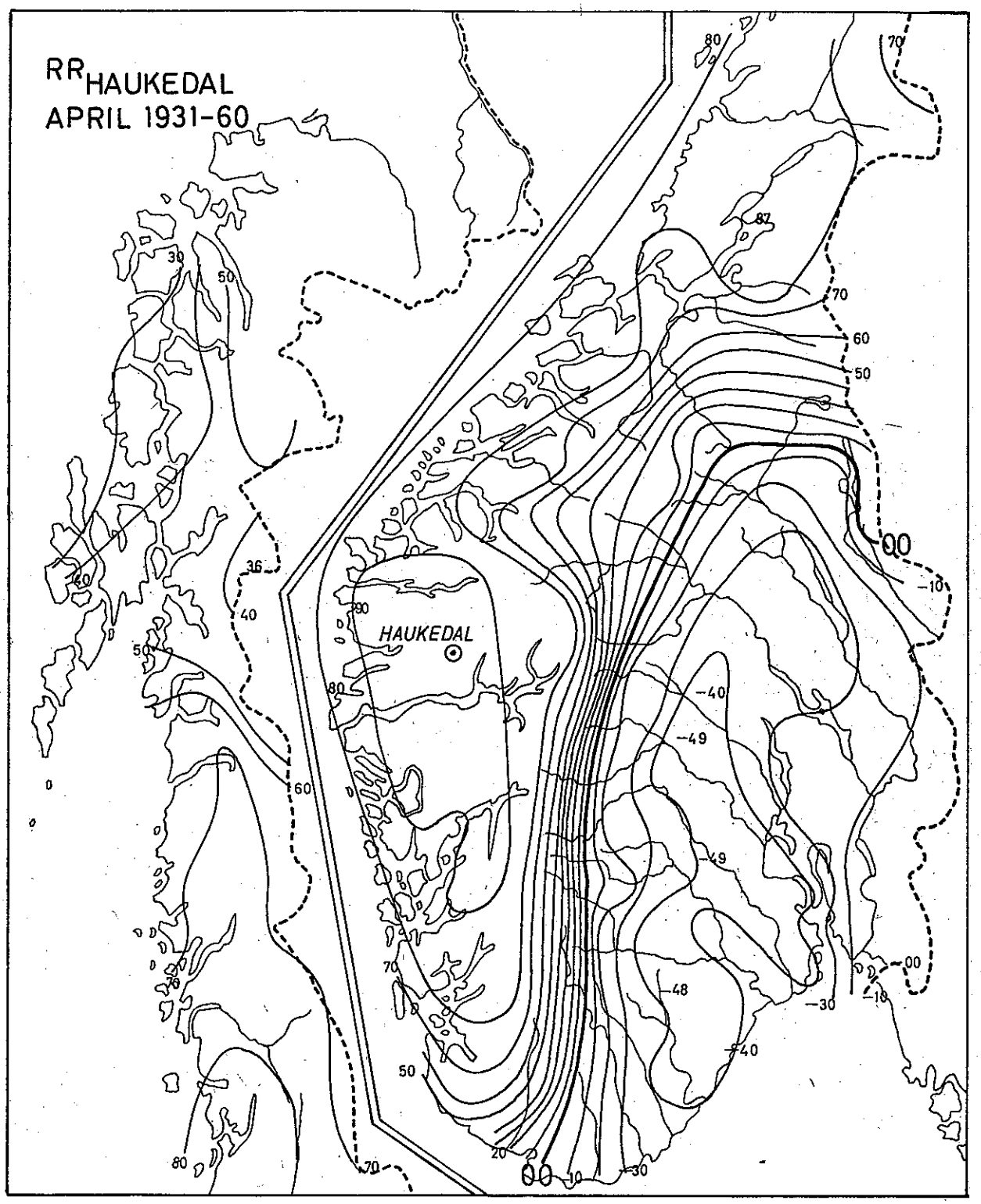


Fig. 32: Space correlation of April precipitation with Haukedal as reference station.

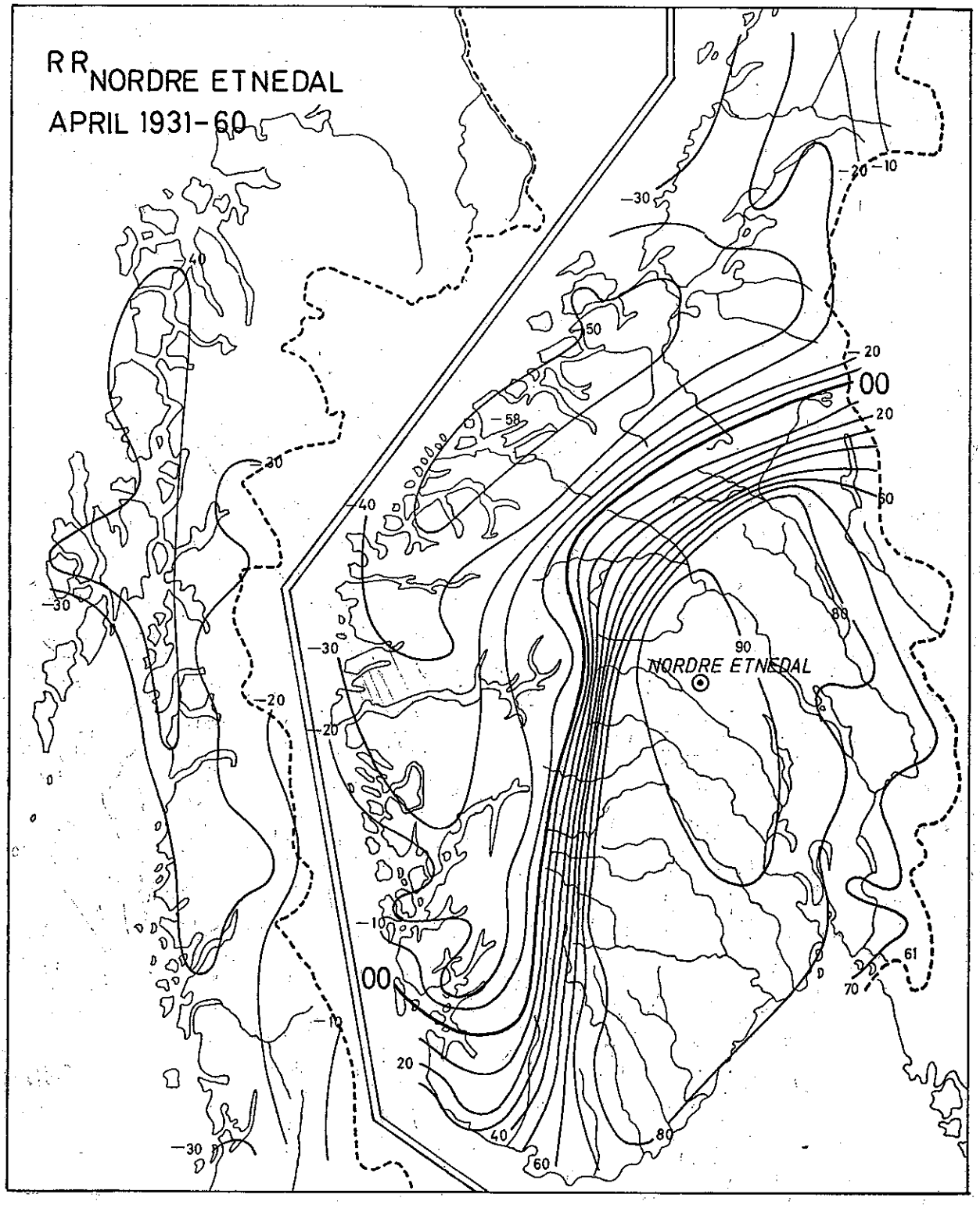


Fig. 33: Space correlation of April precipitation with Nordre Etnedal as reference station.

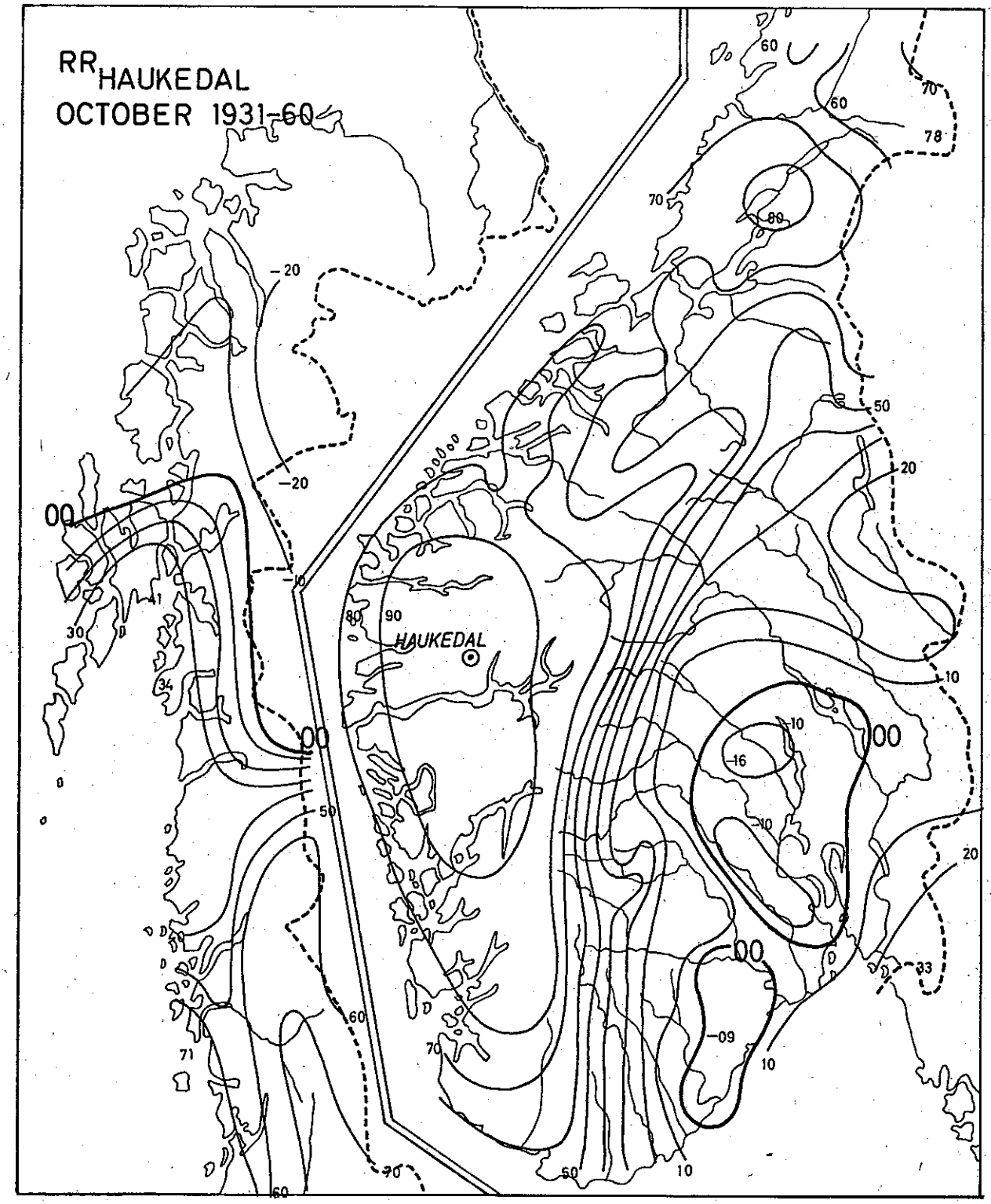


Fig. 34: Space correlation of October precipitation with Haukedal as reference station.

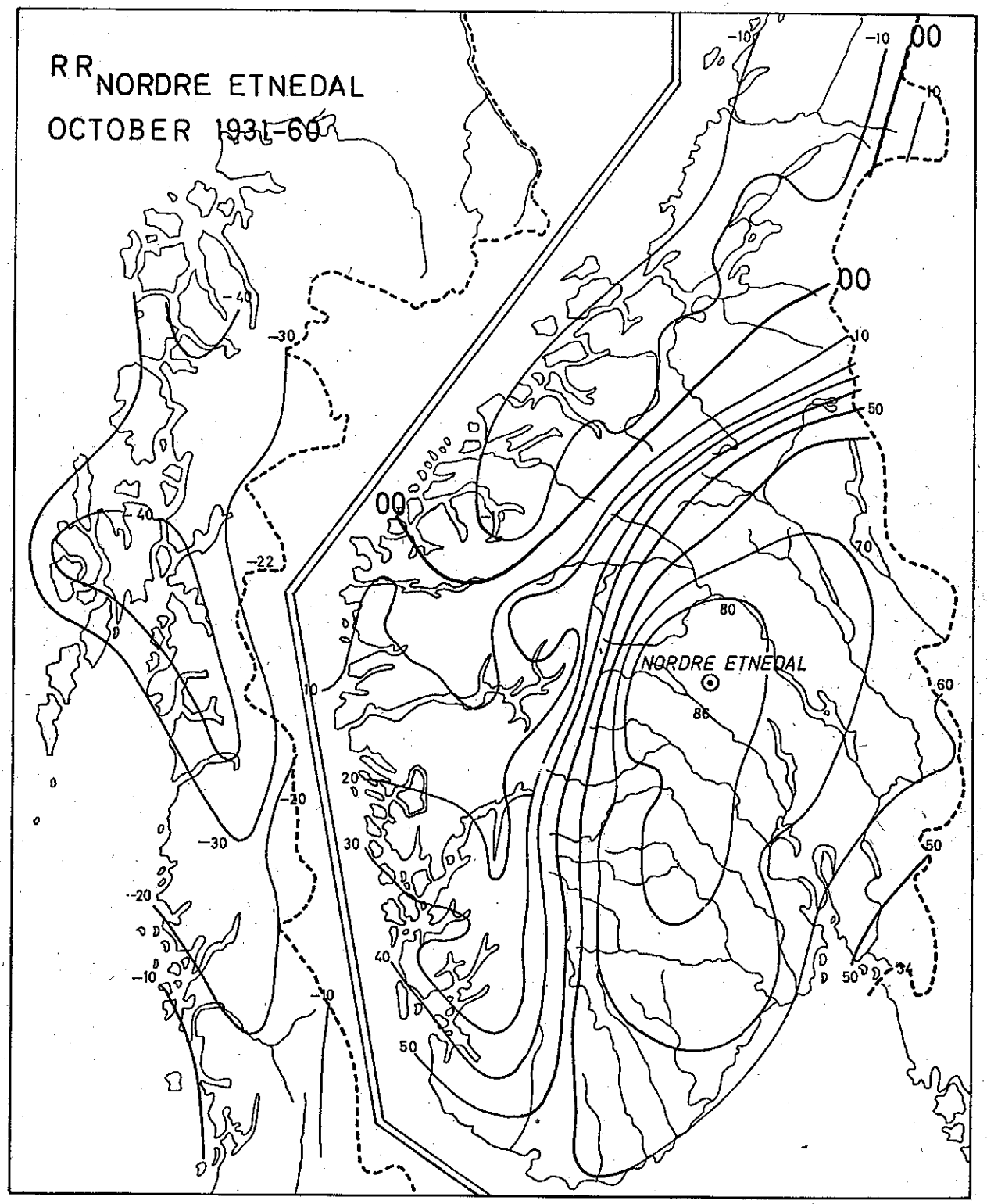


Fig. 35: Space correlation of October precipitation with Nordre Etnedal as reference station.

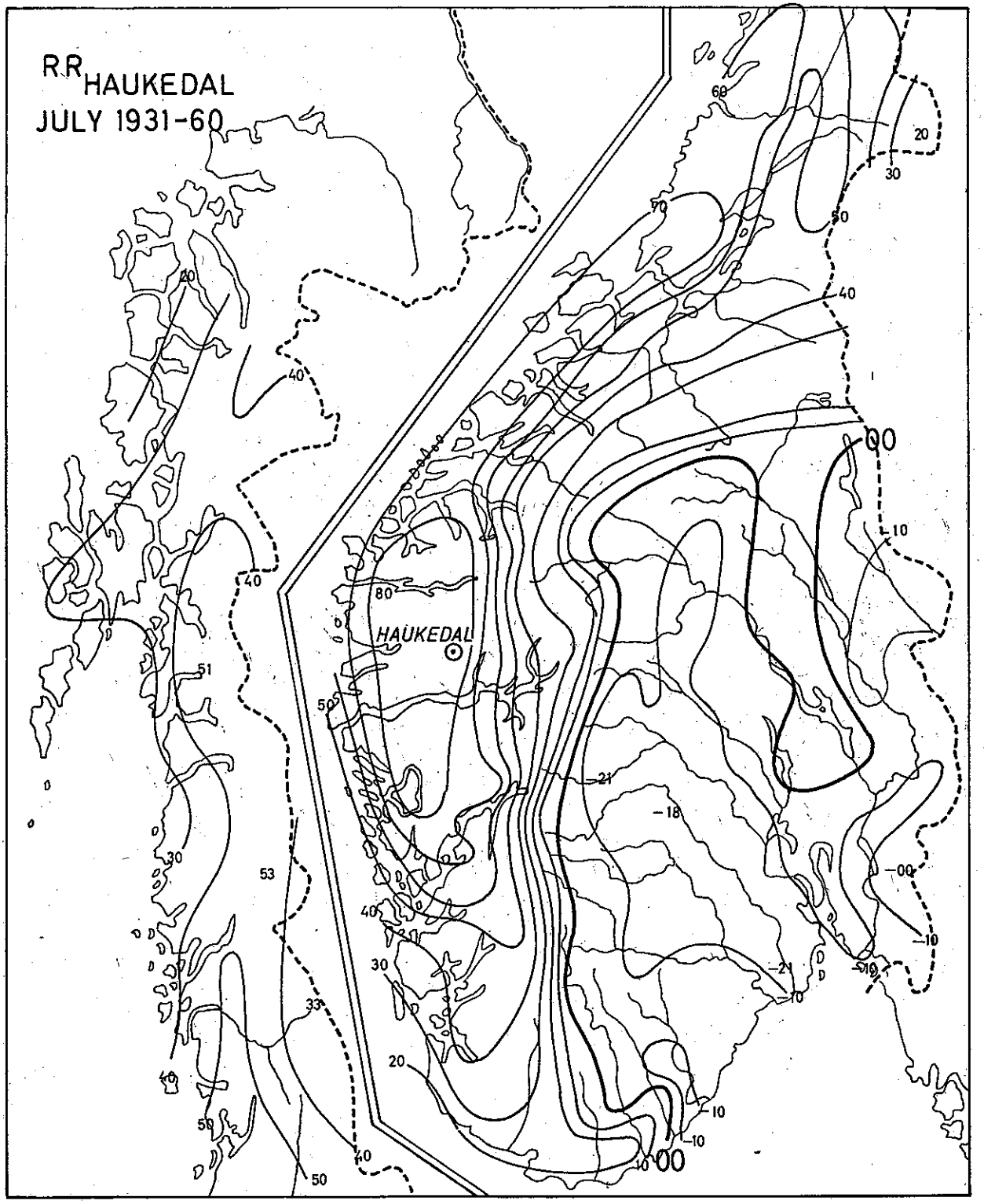


Fig. 36: Space correlation of July rainfall with Haukedal as reference station.

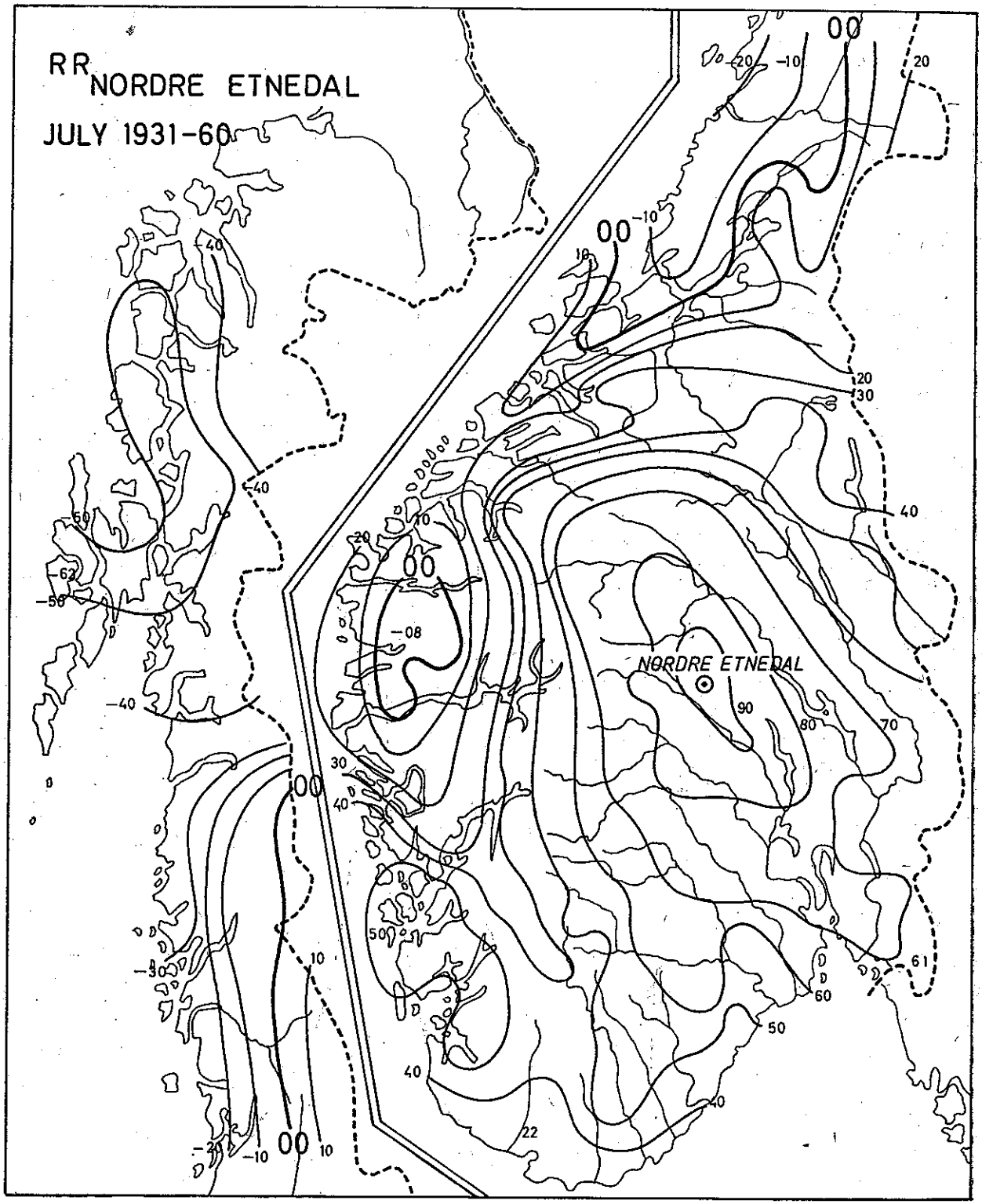


Fig. 37: Space correlation of July rainfall with Nordre Etnedal as reference station.

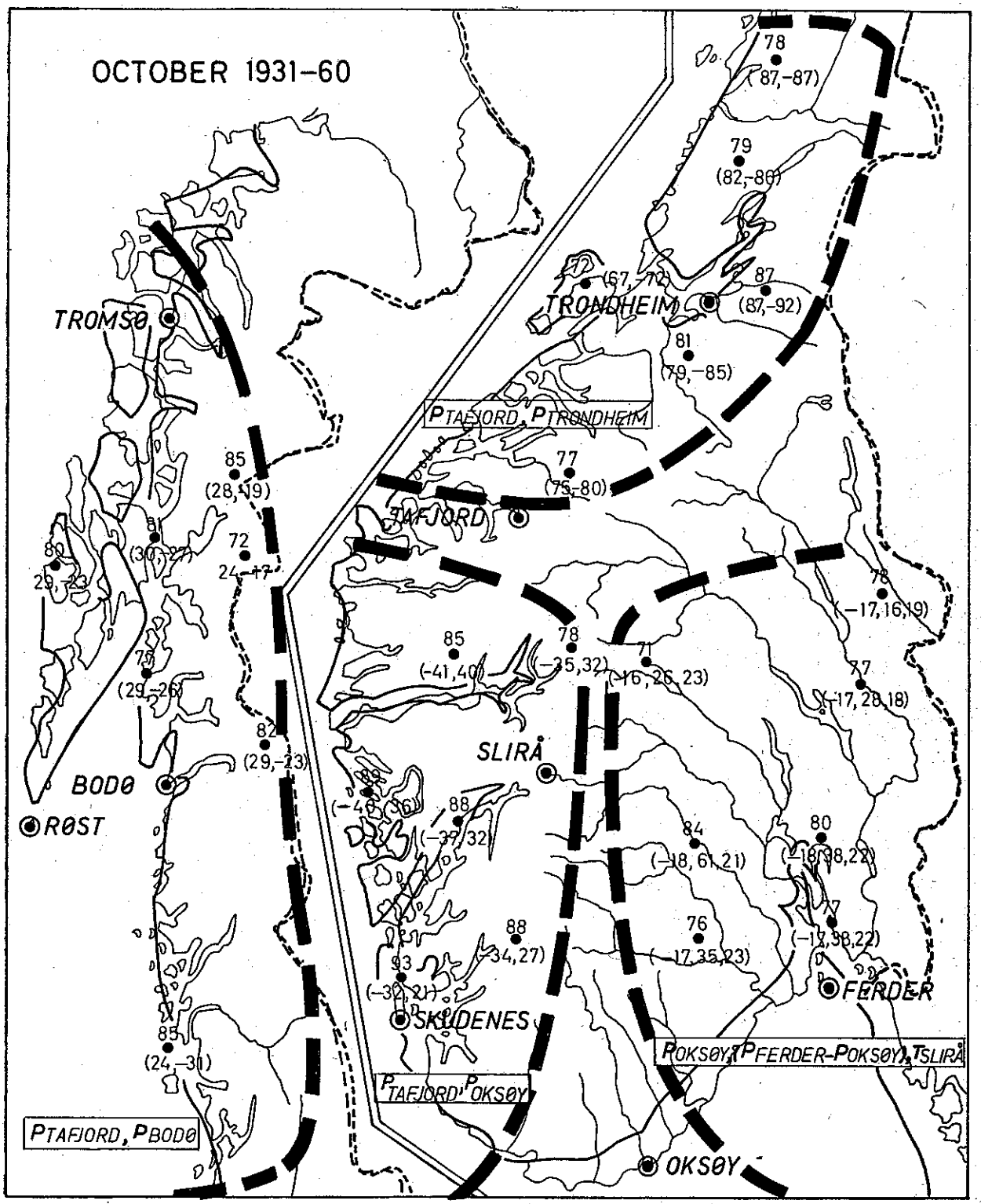


Fig. 38: Specification of standardized precipitation as a function of pressure (mb) and temperature (°C). The weights are in hundredths.

Adding more variables does not raise the explained variance significantly. In eastern Norway, however, three variables are required in order to get multiple correlations close to 0.80. In Fig. 38 the pressure difference ($p_{\text{Tafjord}} - p_{\text{Bodø}}$) specifies precipitation in the northern region as well. In Trøndelag and Møre the coast turns SW to NE, and the difference ($p_{\text{Tafjord}} - p_{\text{Trondheim}}$) is a good estimator of the local precipitation. Proceeding to stations in western Norway, we find in a similar manner that ($p_{\text{Oksøy}} - p_{\text{Tafjord}}$) is well correlated to the precipitation. Consequently our computer runs have proved that the onshore component of the geostrophic wind is an efficient estimator of precipitation over the greater part of Norway. Eastern Norway faces the sea only to the south. The northern part lies in a bowl with highlands to the west, north, and east. The slopes are generally quite modest, and the orographic component is correspondingly weaker. The computer runs also show that three variables must be used in order to derive satisfactory specifications. These three variables are the pressure at Oksøy, the southeasterly geostrophic wind measured by ($p_{\text{Ferder}} - p_{\text{Oksøy}}$), and the temperature $T$ at the mountain station of Slirå. Low pressure, SE wind, and warm air should together provide abundant precipitation in this part of the country.

We also carried out an optimal parameter analysis of precipitation as a function of circulation on a continental scale. We met some difficulties when collecting the data. Some missing observations were interpolated by us, other records had already been interpolated by the foreign agencies. At the end we had a fairly reliable data sample from the period 1881–1930. As independent variables we used monthly mean values of station pressures from the twenty European stations given on Fig. 39. Each station was assigned a number which is placed above the station circle. In brackets are the standard deviations of station pressures in tenths of mm Hg in the months of October and January. These values were approximately equal in Scandinavia. In central and southern parts of Europe the January values are twice as high. In Iceland and western Siberia the ratio is about 1.5.

The computer printed out regression equations of the form

$$\Delta RR = a_i \ \Delta p_i + a_j \ \Delta p_j + a_k \ \Delta p_k + \ldots + e.$$

The symbol $\Delta$ means anomaly (deviation from normal), $RR$ refers to precipitation in mm, $p_i$ is pressure at station $i$ measured in tenths of mm Hg, and $e$ is a random component whose average amplitude depends on the size of the coefficient of multiple correlation.[1] In Table 1 (page 44) are the values of the weights $a_i$, $a_j$, . . for thirty-one stations in Europe. The multiple correlation is given for each equation. We shall interpret two October results in Fig. 40. Boldface weight numbers and streamline refer to the relation for precipitation in Valentia, and thin numbers and streamline refer to precipitation in Aberdeen. In Table 1 the station pressures at 7 (Valentia), 13 (Lisbon), and 20 (Helsinki) give the best relation for the precipitation in Valentia. The weights are given to the right and read as follows: –0.94, 1.11, 0.28. Southwesterly flow should therefore give high values of rainfall in Valentia. Considering next the October rainfall in

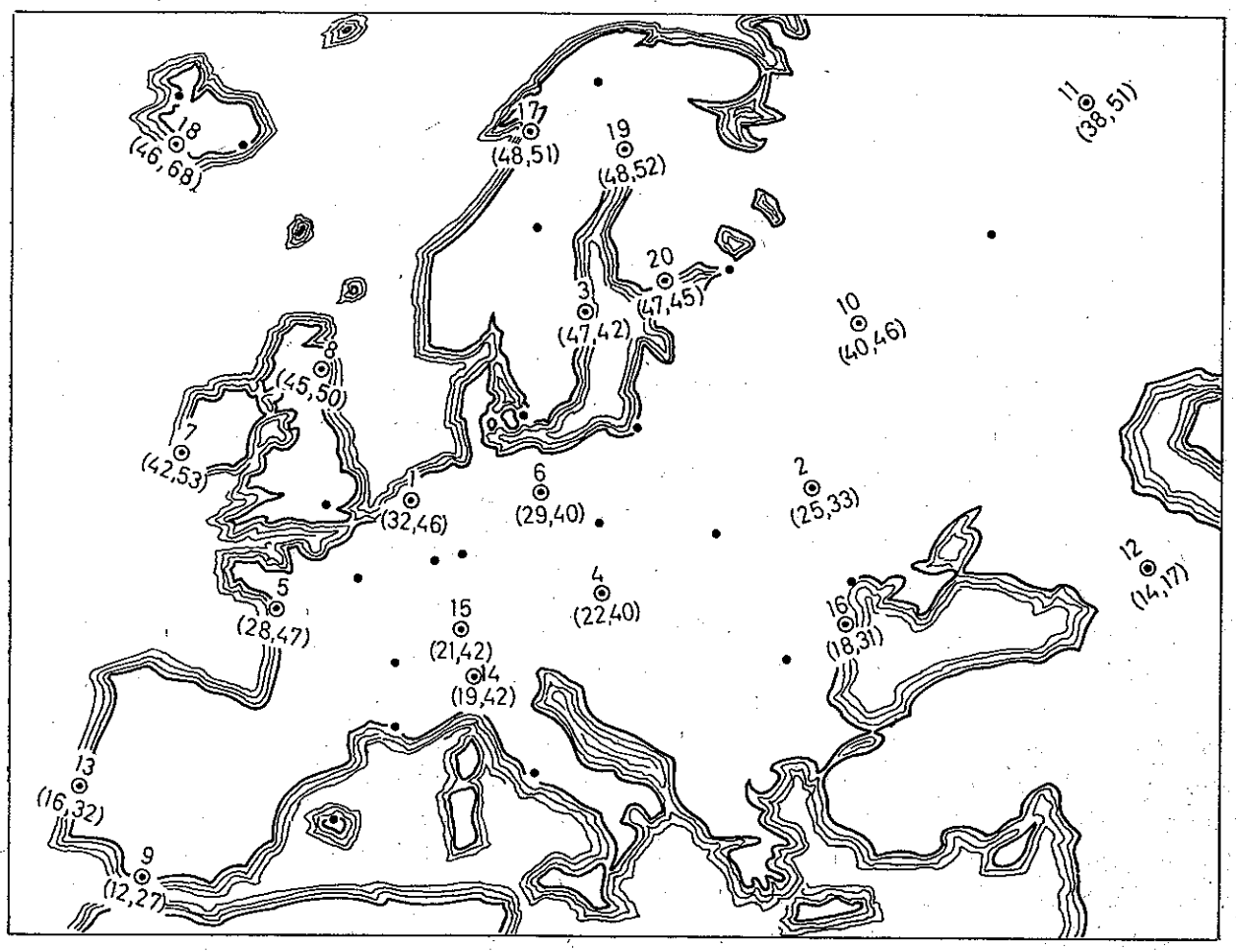


Fig. 39: Location of 20 European reference stations and a specification of October and January values of standard deviation of station pressure in tenths of mm Hg.

Aberdeen we find that the pressure anomalies should be high at stations 18 (Vestmannaeyjar) and 19 (Haparanda) and low in Aberdeen itself. Consequently, Aberdeen precipitation should be high when the flow is easterly. The two samples indicate significant orographic effects, and the reader may find many analogous cases when interpreting the results of Table 1. For example Berlin gets abundant rain when the pressure is low in Central Europe and there is a strong northerly flow between stations 4 (Vienna) and 15 (Zurich). Milan usually has a rainy October when pressure is low on station 5 (Nantes) and high on station 10 (Moscow). As the negative weight on the Nantes pressure is predominant, we may also interpret the result as a requirement of low pressure to the west of Milan, and that southerly winds should prevail between Nantes and Moscow.

Cyclonic circulation over Scandinavia is generally associated with abundant October precipitation in the eastern regions. The weights for Uppsala (station 3) show

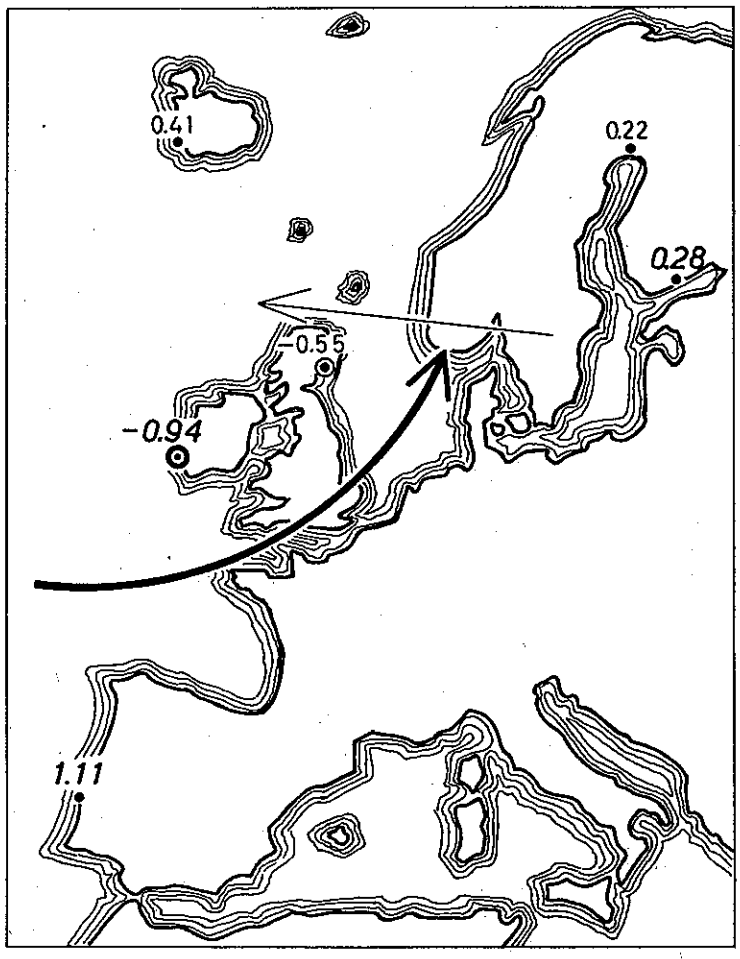


Fig. 40: Optimal weights on station pressures to determine October rainfall in Valentia (boldface figures) and in Aberdeen (thin figures).

that westerly flow between Vienna and Uppsala together with southeasterly wind between Uppsala and Haparanda (station 19) give high estimates. Östersund (Sweden) and Haparanda have similar relationships.

Next we may consider the October precipitation on three Icelandic stations. Vestmannaeyjar (station 18) on the southwestern coast gets usually heavy precipitation when pressures are high at station 7 (Valentia) and station 17 (Bodø) and low at station 18. Southwestern flow in the Atlantic should therefore give a surplus of rain in this part of Iceland. The station Berufjord on the south-eastern coast gets its highest precipitation when there is a strong pressure difference between Bodø and Vestmannaeyjar, i.e., for onshore geostrophic wind. Precipitation on Stykkisholm on the west coast is correlated to a SW to W flow, which is revealed by the weights 0.99 on station 3 pressure, 0.35 on station 7 pressure, and –0.64 on station 17 pressure.

Table 1: Precipitation anomalies (in mm) as a function of pressure distribution (in tenths of mm Hg). The weights are tabulated for the months of October and January.

| Station | Station pressures picked by opt. proc. (numbers as on map in Fig. 39) | | Weights on chosen station pressure anomalies | | Coefficient of mult. corr. | |
|---|---|---|---|---|---|---|
| | October | January | October | January | Oct. | Jan. |
| De Bilt | 6, 13 | 4, 6, 19, 20 | −1.02, 0.68 | 1.06, −1.19, 0.42, −0.45 | 0.85 | 0.77 |
| Frankfurt AM | 6, 18 | 4, 5, 7 | −0.76, −0.21 | −0.54, 0.74, −0.50 | 0.74 | 0.80 |
| Trier | 6, 18 | 4, 5, 7 | −1.04, −0.25 | −0.68, 0.96, −0.64 | 0.81 | 0.78 |
| Berlin | 4, 15 | 6, 11, 15, 17 | −2.06, 1,66 | −1.12, −0.14, 0.94, 0.29 | 0.79 | 0.83 |
| Breslau | 4, 6, 14, 15 | 4, 14, 15 | −4.93, 1.55, 1.27, 1.77 | −0.54, −0.55, 0.93 | 0.62 | 0.78 |
| Vienna | 4, 6, 15 | 4, 5, 19 | −4.53, 1.61, 2.33 | −0.86, 0.61, 0.19 | 0.65 | 0.78 |
| Königsberg | 1, 3, 17 | 15, 19, 20 | 0.60, −1.65, 0.95 | 0.32, 0.60, −0.87 | 0.71 | 0.77 |
| Lvov | 2, 6, 10, 12 | 2, 4, 10 | −2.16, 0.63, 0.76, 0.56 | −0.81, 0.29, 0.33 | 0.70 | 0.72 |
| Bucharest | 8, 10, 16 | 16, 20 | 0.40, 0.35, −1.32 | −0.61, 0.31 | 0.76 | 0.73 |
| Kiev | 2, 11, 18, 20 | 1, 2, 10 | −1.01, 0.22, 0.19, 0.31 | 0.12, −0.80, 0.43 | 0.68 | 0.76 |
| Leningrad | 3, 6, 17 | 16, 19, 20 | −0.86, 0.45, 0.41 | 0.10, 0.33, −0.51 | 0.74 | 0.73 |
| Moscow | 9, 15, 19, 20 | 2, 10, 16 | −0.69, 0.69, 0.89, −1.15 | −0.94, 0.27, 0.43 | 0.69 | 0.71 |
| Kasan | 3, 19, 20 | 2, 7, 16 | 0.71, 0.45, −1.44 | −0.43, −0.07, 0.32 | 0.75 | 0.71 |
| Haparanda | 3, 6, 10 | 9, 11, 17 | −1.03, 0.54, 0.51 | 0.32, 0.18, −0.19 | 0.80 | 0.69 |
| Bodø | 1, 16, 19 | 1, 19 | 0.73, 1.13, −0.76 | 0.61, −0.40 | 0.82 | 0.68 |
| Østersund | 2, 3, 17 | 3, 13, 19 | 0.56, −0.99, 0.43 | −0.29, 0.16, 0.14 | 0.80 | 0.65 |
| Uppsala | 3, 4, 19 | 3, 14, 19 | −1.17, 0.41, 0.75 | −0.51, 0.28, 0.38 | 0.83 | 0.67 |
| Helsinki | 2, 3, 4, 17 | 10, 19, 20 | 0.75, −1.91, 0,50, 1.14 | 0.27, 0.23, −0.67 | 0.79 | 0.71 |
| Copenhagen | 6, 15 | 6, 13 | −1.19, 0.85 | −0.31, 0.42 | 0.78 | 0.77 |
| Aberdeen | 8, 18, 19 | 1, 10, 19 | −0.55, 0,41, 0.22 | −0.29, −0.16, 0.25 | 0.67 | 0.77 |
| Valentia | 7, 13, 20 | 7, 10, 15 | −0.94, 1.11, 0.28 | −1.20, 0.30, 0.83 | 0.79 | 0.90 |
| Greenwich | 1, 7 | 1, 10, 14 | −0.33, −0.38 | −0.64, 0.15, 0.46 | 0.77 | 0.76 |
| Nantes | 1, 5, 15 | 5, 13, 16 | −1.07, −1.76, 1.61 | −1.18, 0.91, 0.34 | 0.90 | 0.86 |
| Paris | 5, 13, 19 | 3, 7, 20 | −1.24, 0.81, −0.31 | −0.64, −0.16, 0.59 | 0.86 | 0.79 |
| Lyon | 5, 12 | 1, 5, 17 | −1.60, 0.91 | −0.75, 0.50, 0.20 | 0.77 | 0.68 |
| Marseille | 12, 15, 16 | 5, 16 | −1.44, −2.08, 2.85 | −0.46, 0.30 | 0.74 | 0.56 |
| Zürich | 1, 5, 14 | 1, 5, 7, 8 | −1.03, 0.62, −0.73 | −1.91, 1.87, −0.84, 0.84 | 0.70 | 0.75 |
| Milan | 5, 10 | 12, 15 | −1.83, 0.70 | +0.69, −0.78 | 0.78 | 0.72 |
| Vestmannaeyjar | 7, 17, 18 | 7, 17, 18 | 0.79, 0.90, −0.82 | 0.56, 0.44, −0.69 | 0.83 | 0.66 |
| Berufjord | 17, 18 | 10, 15, 17, 18 | 0.96, −0.98 | −0.77, 0.65, 1.53, −0.96 | 0.74 | 0.76 |
| Stykkisholm | 3, 7, 17 | 5, 17 | 0.99, 0.35, −0.64 | 0.47, 0.32 | 0.72 | 0.55 |

There are many more interesting features concerning the October precipitation, and the January results are also interesting. But the reader can interpret the remaining results himself and perhaps find results that may be of interest in some particular way. Our intention was to demonstrate that the orographic effects are likely to be very important in most countries throughout the world. Numerical integrations of the equations of motion over a flat surface give prediction skill concerning vertical velocities (of the order cm/sec) on cyclone scales. But forced flow over mountains frequently give vertical velocities that are one order of magnitude greater. As an example, the mountain tilt in eastern Norway is about 1/100, and the slope of the mountain formations facing the Atlantic is approximately 1/40. Onshore winds of 10 m/sec to 20 m/sec should give vertical velocities from 10 cm/sec to 50 cm/sec depending on the slope.

There is no doubt in our minds that we must incorporate the orographic effects in the numerical setups designed for *weather* prediction. But severe problems may arise because of the small scale of many mountain formations. The first practical application may be to convert the predicted fields (by present operational models) to estimates of precipitation and cloud cover by empirical relations of the kind presented in this paper. However, this approach should only be a subsidiary of a much bolder approach. We must sooner or later be able to handle more properly problems concerning motions on scales of less than thousands of kilometers. It should be possible to include such scales in the boundary conditions, also especially in the case of mountains, since the boundary is fixed both in time and space. Some suggestions as to how to proceed should already be available. Our study shows, e.g., that the envelope of the mountain formations may be a fair approximation to the effects on a westerly current across the rugged mountains of western Norway. The stations in the maximum precipitation zone are frequently located near the shores of the narrow fjords, and this fact suggests that the fjord and valley circulations play a secondary role and are usually quite stagnant.

**Acknowledgements.** The authors are indebted to Dr. FJØRTOFT for stimulating discussions when interpreting the statistical results. We are very grateful to Mr. HÅRVIG, who drew the maps and diagrams.

## REFERENCES

AUNE, B., 1966: Personal communication.

BERGERON, T., 1965: On the low-level redistribution of atmospheric water caused by orography. *Proc. of the internat. conf. on cloud physics* (Tokyo and Sapporo).

BIRKELAND, B. J., 1944: Mittel und Extreme der Feuchtigkeit in Norwegen. *Geophysica Norwegica*, **15**, No. 1.

BRUUN, I., 1944: Further synoptic studies on the distribution of precipitation in Southeastern Norway. *Meteorologiske Annaler* **2**, No. 2.

FROGNER, E., 1948: Means and extremes of sea temperature by the Norwegian coast. *Geophysica Norvegica* **15**, No. 3.

HESSELBERG, TH., 1962: Climatological deviation maps. *Geophysica Norvegica* **24**, No. 1.

JOHANSEN, S., 1947: On the distribution of precipitation in Northern Norway in various weather situations. *Meteorologiske Annaler*, **2**, No. 11.

NORDØ, J., 1959: Expected skill of long-range forecasts when derived from daily forecasts and past weather data. *Sc. Rep. No. 4*, Det Norske Meteorologiske Institutt.

— 1960: Significance of regression equations derived from serially correlated data, and a procedure of selecting optimal predictors. *Sp. Rec. No. 8*, Det Norske Meteorologiske Institutt.

— 1964: Varsling av lokale værforhold ved hjelp av korrelasjonsanalyse. *Meddelelser Nr. 17*, Det Danske Meteorologiske Institutt.

— 1966: On empirical deduction of laws from geophysical records. *Sc. Rep. No. 15*, Det Norske Meteorologiske Institutt.

SKAAR, J., 1955: On the measurement of precipitation at sea. *Geophysica Norvegica* **19**, No. 6.

— 1965: Measurement of precipitation on board the ocean weather-ships during the period 1959—1964. Unpublished.

SPINNANGR, F., 1943: Synoptic studies of precipitation in Southern Norway. I. Instability showers. *Meteorologiske Annaler* **1**, No. 12.

— 1943: Synoptic studies of precipitation in Southern Norway, II. Front precipitation. *Meteorologiske Annaler* **1**, No. 17.

— and H. JOHANSEN, 1954: On the distribution of precipitation in maritime tropical air over Norway. *Meteorologiske Annaler* **3**, No. 14.

— — , 1955: On the influence of the orography in Southern Norway on instability showers from the sea. *Meteorologiske Annaler* **4**, No. 3.

Avhandlinger som ønskes opptatt i «Geofysiske Publikasjoner», må fremlegges i Videnskaps-Akademiet av et sakkyndig medlem.

**Vol. XXII.**

No. 1. L. Harang and K. Malmjord: Drift measurements of the E-layer at Kjeller and Tromsø during the international geophysical year 1957—58. 1960.
» 2. Leiv Harang and Anders Omholt: Luminosity curves of high aurorae. 1960.
» 3. Arnt Eliassen and Enok Palm: On the transler of energy in stationary mountain waves. 1961.
» 4. Yngvar Gotaas: Mother of pearl clouds over Southern Norway, February 21, 1959. 1961.
» 5. H. Økland: An experiment in numeral integration of the barotropic equation by a quasi-Lagrangian method. 1962.
» 6. L. Vegard: Auroral investigations during the winter seasons 1957/58—1959/60 and their bearing on solar terrestrial relationships. 1961.
» 7. Gunnvald Bøyum: A study of evaporation and heat exchange between the sea surface and the atmosphere. 1962.

**Vol. XXIII.**

No. 1. Bernt Mæhlum: The sporadic E auroral zone. 1962.
» 2. Bernt Mæhlum: Small scale structure and drift in the sporadic E layer as observed in the auroral zone. 1962.
» 3. L. Harang and K. Malmjord: Determination of drift movements of the ionosphere at high latitudes from radio star scintillations. 1962.
» 4. Eyvind Riis: The stability of Couette-flow in non-stratified and stratified viscous fluids. 1962.
» 5. E. Frogner: Temperature changes on a large scale in the arctic winter stratosphere and their probable effects on the tropospheric circulation. 1962.
» 6. Odd H. Sælen: Studies in the Norwegian Atlantic Current. Part II: Investigations during the years 1954—59 in an area west of Stad. 1963.

**Vol. XXIV.**

In memory of Vilhelm Bjerknes on the 100th anniversary of his birth. 1962.

**Vol. XXV.**

No. 1. Kaare Pedersen: On the quantitative precipitation forecasting with a quasi-geostrophic model. 1963.
» 2. Peter Thrane: Perturbations in a baroclinic model atmosphere. 1963.
» 3. Eigil Hesstvedt: On the water vapor content in the high atmosphere. 1964.
» 4. Torbjørn Ellingsen: On periodic motions of an ideal fluid with an elastic boundary. 1964.
» 5. Jonas Ekman Fjeldstad: Internal waves of tidal origin. 1964.
» 6. A. Eftestøl and A. Omholt: Studies on the excitation of $N_2$ and $N_2^+$ band sin aurora. 1965.

**Vol. XXVI.**

No. 1. Eigil Hesstvedt: Some characteristics of the oxygen-hydrogen atmosphere. 1965.
» 2. William Blumen: A random model of momentum flux by mountain waves. 1965.
» 3. K. M. Storetvedt: Remanent magnetization of some dolerite intrusions in the Egersund Area, Southern Norway. 1966.
» 4. Martin Mork: The generation of surface waves by wind and their propagation from a storm area. 1966.
» 5. Jack Nordø: The vertical structure of the atmosphere. 1965.
» 6. Alv Egeland and Anders Omholt: Carl Størmer's height measurements of aurora. 1966.
» 7. Gunnvald Bøyum: The energy exchange between sea and atmosphere at ocean weather stations M, I and A. 1966.
» 8. Torbjørn Ellingsen and Enok Palm: The energy transfer from submarine seismic waves to the ocean. 1966.
» 9. Torkild Carstens: Experiments with supercooling and ice formation in flowing water. 1966.
» 10. Jørgen Holmboe: On the instability of stratified shear flow. 1966.
» 11. Lawrence H. Larsen: Flow over obstacles of finite amplitude. 1966.

A.s John Griegs Boktrykkeri